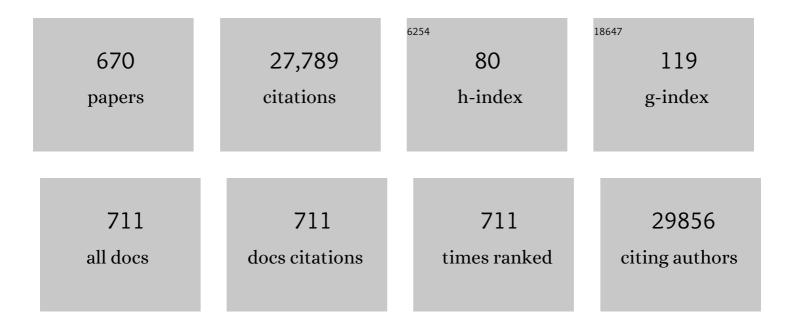
List of Publications by Year in descending order

Source: https://exaly.com/author-pdf/7083221/publications.pdf Version: 2024-02-01



#	Article	IF	CITATIONS
1	New Synthetic Routes to Alkyl Monolayers on the Si(111) Surface1. Langmuir, 1999, 15, 3831-3835.	3.5	315
2	Surface plasmon resonance-based biosensors: From the development of different SPR structures to novel surface functionalization strategies. Current Opinion in Solid State and Materials Science, 2011, 15, 208-224.	11.5	295
3	Wettability Switching Techniques on Superhydrophobic Surfaces. Nanoscale Research Letters, 2007, 2,	5.7	289
4	Preparation of Superhydrophobic Coatings on Zinc as Effective Corrosion Barriers. ACS Applied Materials & Interfaces, 2009, 1, 1150-1153.	8.0	285
5	Sensing using localised surface plasmon resonance sensors. Chemical Communications, 2012, 48, 8999.	4.1	266
6	Cu-Ag bimetallic nanoparticles on reduced graphene oxide nanosheets as peroxidase mimic for glucose and ascorbic acid detection. Sensors and Actuators B: Chemical, 2017, 238, 842-851.	7.8	259
7	Facile synthesis of fluorinated polydopamine/chitosan/reduced graphene oxide composite aerogel for efficient oil/water separation. Chemical Engineering Journal, 2017, 326, 17-28.	12.7	255
8	Antibacterial activity of graphene-based materials. Journal of Materials Chemistry B, 2016, 4, 6892-6912.	5.8	246
9	Polyurethane sponge functionalized with superhydrophobic nanodiamond particles for efficient oil/water separation. Chemical Engineering Journal, 2017, 307, 319-325.	12.7	237
10	Functional Carbon Quantum Dots as Medical Countermeasures to Human Coronavirus. ACS Applied Materials & Interfaces, 2019, 11, 42964-42974.	8.0	231
11	Reversible Electrowetting on Superhydrophobic Silicon Nanowires. Nano Letters, 2007, 7, 813-817.	9.1	225
12	Sunlight-driven water-splitting using two-dimensional carbon based semiconductors. Journal of Materials Chemistry A, 2018, 6, 12876-12931.	10.3	215
13	Controlled Functionalization and Multistep Chemical Manipulation of Covalently Modified Si(111) Surfaces1. Journal of the American Chemical Society, 1999, 121, 11513-11515.	13.7	212
14	Insights into the Formation Mechanisms of Siâ^'OR Monolayers from the Thermal Reactions of Alcohols and Aldehydes with Si(111)â^'H1. Langmuir, 2000, 16, 7429-7434.	3.5	199
15	A green and sensitive guanine-based DNA biosensor for idarubicin anticancer monitoring in biological samples: A simple and fast strategy for control of health quality in chemotherapy procedure confirmed by docking investigation. Chemosphere, 2022, 291, 132928.	8.2	194
16	Recent advances in the development of graphene-based surface plasmon resonance (SPR) interfaces. Analytical and Bioanalytical Chemistry, 2013, 405, 1435-1443.	3.7	191
17	Carbon-based quantum particles: an electroanalytical and biomedical perspective. Chemical Society Reviews, 2019, 48, 4281-4316.	38.1	187
18	Reduction and Functionalization of Graphene Oxide Sheets Using Biomimetic Dopamine Derivatives in One Step. ACS Applied Materials & Interfaces, 2012, 4, 1016-1020.	8.0	182

#	Article	IF	CITATIONS
19	Different strategies for functionalization of diamond surfaces. Journal of Solid State Electrochemistry, 2008, 12, 1205-1218.	2.5	180
20	Electrochemical Methodologies for the Detection of Pathogens. ACS Sensors, 2018, 3, 1069-1086.	7.8	178
21	Thermal Hydrosilylation of Undecylenic Acid with Porous Silicon. Journal of the Electrochemical Society, 2002, 149, H59.	2.9	177
22	Well-Defined Carboxyl-Terminated Alkyl Monolayers Grafted onto Hâ^'Si(111):Â Packing Density from a Combined AFM and Quantitative IR Study. Langmuir, 2006, 22, 153-162.	3.5	172
23	Formation, Characterization, and Chemistry of Undecanoic Acid-Terminated Silicon Surfaces:Â Patterning and Immobilization of DNA. Langmuir, 2004, 20, 11713-11720.	3.5	171
24	Recent advances in surface chemistry strategies for the fabrication of functional iron oxide based magnetic nanoparticles. Nanoscale, 2013, 5, 10729.	5.6	164
25	Reduced graphene oxide decorated with Co3O4 nanoparticles (rGO-Co3O4) nanocomposite: A reusable catalyst for highly efficient reduction of 4-nitrophenol, and Cr(VI) and dye removal from aqueous solutions. Chemical Engineering Journal, 2017, 322, 375-384.	12.7	160
26	The preparation of flat H–Si(111) surfaces in 40% NH4F revisited. Electrochimica Acta, 2000, 45, 4591-4598.	5.2	157
27	Reduced graphene oxide nanosheets decorated with Au, Pd and Au–Pd bimetallic nanoparticles as highly efficient catalysts for electrochemical hydrogen generation. Journal of Materials Chemistry A, 2015, 3, 20254-20266.	10.3	146
28	Gold–graphene nanocomposites for sensing and biomedical applications. Journal of Materials Chemistry B, 2015, 3, 4301-4324.	5.8	144
29	Preparation of magnetic, superhydrophobic/superoleophilic polyurethane sponge: Separation of oil/water mixture and demulsification. Chemical Engineering Journal, 2020, 384, 123339.	12.7	144
30	Ideal Passivation of Luminescent Porous Silicon by Thermal, Noncatalytic Reaction with Alkenes and Aldehydesâ€. Chemistry of Materials, 2001, 13, 2002-2011.	6.7	139
31	The synthesis of citrate-modified silver nanoparticles in an aqueous suspension of graphene oxide nanosheets and their antibacterial activity. Colloids and Surfaces B: Biointerfaces, 2013, 105, 128-136.	5.0	137
32	Green chemistry approach for the synthesis of ZnO–carbon dots nanocomposites with good photocatalytic properties under visible light. Journal of Colloid and Interface Science, 2016, 465, 286-294.	9.4	137
33	Chemical reactivity of hydrogen-terminated crystalline silicon surfaces. Current Opinion in Solid State and Materials Science, 2005, 9, 66-72.	11.5	133
34	Silicon Nanowires Coated with Silver Nanostructures as Ultrasensitive Interfaces for Surface-Enhanced Raman Spectroscopy. ACS Applied Materials & Interfaces, 2009, 1, 1396-1403.	8.0	133
35	Towards green synthesis of monodisperse Cu nanoparticles: An efficient and high sensitive electrochemical nitrite sensor. Sensors and Actuators B: Chemical, 2018, 266, 873-882.	7.8	133
36	PdCl2-Catalyzed Reduction of Organic Halides by Triethylsilane. Organometallics, 1996, 15, 1508-1510.	2.3	132

#	Article	IF	CITATIONS
37	Preparation of reduced graphene oxide–Ni(OH) <sub>2</sub> composites by electrophoretic deposition: application for non-enzymatic glucose sensing. Journal of Materials Chemistry A, 2014, 2, 5525-5533.	10.3	128
38	Microwave-Assisted Chemical Functionalization of Hydrogen-Terminated Porous Silicon Surfaces. Journal of Physical Chemistry B, 2003, 107, 13459-13462.	2.6	125
39	Lysozyme detection on aptamer functionalized graphene-coated SPR interfaces. Biosensors and Bioelectronics, 2013, 50, 239-243.	10.1	125
40	Nickel Decorated on Phosphorous-Doped Carbon Nitride as an Efficient Photocatalyst for Reduction of Nitrobenzenes. Nanomaterials, 2016, 6, 59.	4.1	121
41	Matrix-Free Laser Desorption/Ionization Mass Spectrometry on Silicon Nanowire Arrays Prepared by Chemical Etching of Crystalline Silicon. Langmuir, 2010, 26, 1354-1361.	3.5	118
42	Eco-friendly synthesis of ZnO nanoparticles with different morphologies and their visible light photocatalytic performance for the degradation of Rhodamine B. Ceramics International, 2016, 42, 10259-10265.	4.8	116
43	Iron oxide magnetic nanoparticles with versatile surface functions based on dopamine anchors. Nanoscale, 2013, 5, 2692.	5.6	114
44	MoS2/reduced graphene oxide as active hybrid material for the electrochemical detection of folic acid in human serum. Biosensors and Bioelectronics, 2016, 85, 807-813.	10.1	113
45	High Efficiency of Functional Carbon Nanodots as Entry Inhibitors of Herpes Simplex Virus Type 1. ACS Applied Materials & Interfaces, 2016, 8, 9004-9013.	8.0	112
46	Preparation of Superhydrophobic Silicon Oxide Nanowire Surfaces. Langmuir, 2007, 23, 1608-1611.	3.5	111
47	Core–shell structured reduced graphene oxide wrapped magnetically separable rGO@CuZnO@Fe3O4 microspheres as superior photocatalyst for CO2 reduction under visible light. Applied Catalysis B: Environmental, 2017, 205, 654-665.	20.2	111
48	Electrochemical Aptamer-Based Biosensors for the Detection of Cardiac Biomarkers. ACS Omega, 2018, 3, 12010-12018.	3.5	111
49	Graphene-based biosensors. Interface Focus, 2018, 8, 20160132.	3.0	110
50	Culture of mammalian cells on patterned superhydrophilic/superhydrophobic silicon nanowire arrays. Soft Matter, 2011, 7, 8642.	2.7	109
51	Cellulose Nanocrystals/Graphene Hybrids—A Promising New Class of Materials for Advanced Applications. Nanomaterials, 2020, 10, 1523.	4.1	109
52	Sensitive electrochemical detection of cardiac troponin I in serum and saliva by nitrogen-doped porous reduced graphene oxide electrode. Sensors and Actuators B: Chemical, 2018, 262, 180-187.	7.8	108
53	Highly Sensitive Detection of DNA Hybridization on Commercialized Graphene-Coated Surface Plasmon Resonance Interfaces. Analytical Chemistry, 2014, 86, 11211-11216.	6.5	106
54	Nanostructures for the Inhibition of Viral Infections. Molecules, 2015, 20, 14051-14081.	3.8	104

#	Article	IF	CITATIONS
55	Label-free femtomolar cancer biomarker detection in human serum using graphene-coated surface plasmon resonance chips. Biosensors and Bioelectronics, 2017, 89, 606-611.	10.1	104
56	Efficient and Durable Oxygen Reduction Electrocatalyst Based on CoMn Alloy Oxide Nanoparticles Supported Over N-Doped Porous Graphene. ACS Catalysis, 2017, 7, 6700-6710.	11.2	104
57	Quantitative Testing of Robustness on Superomniphobic Surfaces by Drop Impact. Langmuir, 2010, 26, 18369-18373.	3.5	102
58	Glycan-functionalized diamond nanoparticles as potent E. coli anti-adhesives. Nanoscale, 2013, 5, 2307.	5.6	102
59	Inorganic Molybdenum Octahedral Nanosized Cluster Units, Versatile Functional Building Block for Nanoarchitectonics. Journal of Inorganic and Organometallic Polymers and Materials, 2015, 25, 189-204.	3.7	102
60	Ag and Au nanoparticles/reduced graphene oxide composite materials: Synthesis and application in diagnostics and therapeutics. Advances in Colloid and Interface Science, 2019, 271, 101991.	14.7	102
61	Preparation of boron-doped diamond nanowires and their application for sensitive electrochemical detection of tryptophan. Electrochemistry Communications, 2010, 12, 438-441.	4.7	101
62	Preparation of reduced graphene oxide/Cu nanoparticle composites through electrophoretic deposition: application for nonenzymatic glucose sensing. RSC Advances, 2015, 5, 15861-15869.	3.6	100
63	Structural and optical properties of Na doped ZnO nanocrystals: Application to solar photocatalysis. Applied Surface Science, 2017, 396, 1528-1538.	6.1	99
64	Cellular and in vivo toxicity of functionalized nanodiamond in Xenopus embryos. Journal of Materials Chemistry, 2010, 20, 8064.	6.7	98
65	Enhanced antibacterial activity of carbon dots functionalized with ampicillin combined with visible light triggered photodynamic effects. Colloids and Surfaces B: Biointerfaces, 2018, 170, 347-354.	5.0	98
66	Direct Functionalization of Nanodiamond Particles Using Dopamine Derivatives. Langmuir, 2011, 27, 12451-12457.	3.5	94
67	Magnetic polyurethane sponge for efficient oil adsorption and separation of oil from oil-in-water emulsions. Separation and Purification Technology, 2020, 240, 116627.	7.9	93
68	How the Intricate Interactions between Carbon Nanotubes and Two Bilirubin Oxidases Control Direct and Mediated O <sub>2</sub> Reduction. ACS Applied Materials & Interfaces, 2016, 8, 23074-23085.	8.0	91
69	Stabilization of porous silicon electroluminescence by surface passivation with controlled covalent bonds. Applied Physics Letters, 2003, 83, 2342-2344.	3.3	89
70	PMS activation using reduced graphene oxide under sonication: Efficient metal-free catalytic system for the degradation of rhodamine B, bisphenol A, and tetracycline. Ultrasonics Sonochemistry, 2019, 52, 164-175.	8.2	89
71	NiFe layered double hydroxide electrodeposited on Ni foam coated with reduced graphene oxide for high-performance supercapacitors. Electrochimica Acta, 2019, 302, 1-9.	5.2	89
72	Thermal Route for Chemical Modification and Photoluminescence Stabilization of Porous Silicon. Physica Status Solidi A, 2000, 182, 117-121.	1.7	88

#	Article	IF	CITATIONS
73	Plasmonic photothermal destruction of uropathogenic E. coli with reduced graphene oxide and core/shell nanocomposites of gold nanorods/reduced graphene oxide. Journal of Materials Chemistry B, 2015, 3, 375-386.	5.8	88
74	Facile synthesis and characterization of a novel 1,2,4,5-benzene tetracarboxylic acid doped polyaniline@zinc phosphate nanocomposite for highly efficient removal of hazardous hexavalent chromium ions from water. Journal of Colloid and Interface Science, 2021, 585, 560-573.	9.4	87
75	Photochemical oxidation of hydrogenated boron-doped diamond surfaces. Electrochemistry Communications, 2005, 7, 937-940.	4.7	86
76	Reduced graphene oxide/polyethylenimine based immunosensor for the selective and sensitive electrochemical detection of uropathogenic Escherichia coli. Sensors and Actuators B: Chemical, 2018, 260, 255-263.	7.8	86
77	The antimicrobial effect of silicon nanowires decorated with silver and copper nanoparticles. Nanotechnology, 2013, 24, 495101.	2.6	85
78	Gold island films on indium tin oxide for localized surface plasmon sensing. Nanotechnology, 2008, 19, 195712.	2.6	84
79	Synthesis and characterization of arginine-doped polyaniline/walnut shell hybrid composite with superior clean-up ability for chromium (VI) from aqueous media: Equilibrium, reusability and process optimization. Journal of Molecular Liquids, 2020, 316, 113832.	4.9	84
80	Engineering Sticky Superomniphobic Surfaces on Transparent and Flexible PDMS Substrate. Langmuir, 2010, 26, 17242-17247.	3.5	83
81	Surface plasmon resonance: signal amplification using colloidal gold nanoparticles for enhanced sensitivity. Reviews in Analytical Chemistry, 2014, 33, .	3.2	83
82	Extreme Resistance of Superhydrophobic Surfaces to Impalement: Reversible Electrowetting Related to the Impacting/Bouncing Drop Test. Langmuir, 2008, 24, 11203-11208.	3.5	82
83	Nucleic aptamer modified porous reduced graphene oxide/MoS2 based electrodes for viral detection: Application to human papillomavirus (HPV). Sensors and Actuators B: Chemical, 2018, 262, 991-1000.	7.8	82
84	Functionalization of Azide-Terminated Silicon Surfaces with Glycans Using Click Chemistry: XPS and FTIR Study. Journal of Physical Chemistry C, 2013, 117, 368-375.	3.1	81
85	EWOD driven cleaning of bioparticles on hydrophobic and superhydrophobic surfaces. Lab on A Chip, 2011, 11, 490-496.	6.0	80
86	Solvothermal synthesis of CoS/reduced porous graphene oxide nanocomposite for selective colorimetric detection of Hg(II) ion in aqueous medium. Sensors and Actuators B: Chemical, 2017, 244, 684-692.	7.8	80
87	Magnetically driven superhydrophobic/superoleophilic graphene-based polyurethane sponge for highly efficient oil/water separation and demulsification. Separation and Purification Technology, 2021, 274, 118931.	7.9	80
88	Comparison of the chemical composition of boron-doped diamond surfaces upon different oxidation processes. Electrochimica Acta, 2009, 54, 5818-5824.	5.2	79
89	Heat: A Highly Efficient Skin Enhancer for Transdermal Drug Delivery. Frontiers in Bioengineering and Biotechnology, 2018, 6, 15.	4.1	79
90	Preparation of Superhydrophobic Coatings on Zinc, Silicon, and Steel by a Solution-Immersion Technique. ACS Applied Materials & Interfaces, 2009, 1, 2086-2091.	8.0	78

#	Article	IF	CITATIONS
91	One-pot synthesis of gold nanoparticle/molybdenum cluster/graphene oxide nanocomposite and its photocatalytic activity. Applied Catalysis B: Environmental, 2013, 130-131, 270-276.	20.2	78
92	Graphene oxide chemically reduced and functionalized with KOH-PEI for efficient Cr(VI) adsorption and reduction in acidic medium. Chemosphere, 2020, 258, 127316.	8.2	77
93	Surface Plasmon Resonance Investigation of Silver and Gold Films Coated with Thin Indium Tin Oxide Layers: Influence on Stability and Sensitivity. Journal of Physical Chemistry C, 2008, 112, 15813-15817.	3.1	76
94	Diamond nanowires for highly sensitive matrix-free mass spectrometry analysis of small molecules. Nanoscale, 2012, 4, 231-238.	5.6	75
95	Fast photocatalytic degradation of rhodamine B over [Mo6Br8(N3)6]2â^' cluster units under sun light irradiation. Applied Catalysis B: Environmental, 2012, 123-124, 1-8.	20.2	75
96	Reduced Graphene-Oxide-Embedded Polymeric Nanofiber Mats: An "On-Demand―Photothermally Triggered Antibiotic Release Platform. ACS Applied Materials & Interfaces, 2018, 10, 41098-41106.	8.0	75
97	High sensitive matrix-free mass spectrometry analysis of peptides using silicon nanowires-based digital microfluidic device. Lab on A Chip, 2011, 11, 1620.	6.0	74
98	Zipping Effect on Omniphobic Surfaces for Controlled Deposition of Minute Amounts of Fluid or Colloids. Small, 2012, 8, 1229-1236.	10.0	74
99	Stability Enhancement of Partially-Oxidized Porous Silicon Nanostructures Modified with Ethyl Undecylenate. Nano Letters, 2001, 1, 713-717.	9.1	73
100	Sulfonated reduced graphene oxide as a highly efficient catalyst for direct amidation of carboxylic acids with amines using ultrasonic irradiation. Ultrasonics Sonochemistry, 2016, 29, 371-379.	8.2	73
101	Tip-Enhanced Raman Spectroscopy of Combed Double-Stranded DNA Bundles. Journal of Physical Chemistry C, 2014, 118, 1174-1181.	3.1	72
102	Magnetic reduced graphene oxide loaded hydrogels: Highly versatile and efficient adsorbents for dyes and selective Cr(VI) ions removal. Journal of Colloid and Interface Science, 2017, 507, 360-369.	9.4	72
103	Cobalt phthalocyanine-supported reduced graphene oxide: A highly efficient catalyst for heterogeneous activation of peroxymonosulfate for rhodamine B and pentachlorophenol degradation. Chemical Engineering Journal, 2018, 336, 465-475.	12.7	72
104	CoO Promoted the Catalytic Activity of Nitrogen-Doped MoS <sub>2</sub> Supported on Carbon Fibers for Overall Water Splitting. ACS Applied Materials & Interfaces, 2019, 11, 31889-31898.	8.0	72
105	Fabrication of ZnCoS nanomaterial for high energy flexible asymmetric supercapacitors. Chemical Engineering Journal, 2019, 374, 347-358.	12.7	72
106	Functionalization of Diamond Nanoparticles Using "Click―Chemistry. Langmuir, 2010, 26, 13168-13172.	3.5	71
107	Synthesis and photocatalytic activity of iodine-doped ZnO nanoflowers. Journal of Materials Chemistry, 2011, 21, 10982.	6.7	71
108	Silicon nanowire arrays-induced graphene oxide reduction under UV irradiation. Nanoscale, 2011, 3, 4662.	5.6	71

#	Article	IF	CITATIONS
109	Phenylboronic-Acid-Modified Nanoparticles: Potential Antiviral Therapeutics. ACS Applied Materials & Interfaces, 2013, 5, 12488-12498.	8.0	71
110	Cobalt phthalocyanine tetracarboxylic acid modified reduced graphene oxide: a sensitive matrix for the electrocatalytic detection of peroxynitrite and hydrogen peroxide. RSC Advances, 2015, 5, 1474-1484.	3.6	70
111	Plasmonic photothermal cancer therapy with gold nanorods/reduced graphene oxide core/shell nanocomposites. RSC Advances, 2016, 6, 1600-1610.	3.6	70
112	Photothermally triggered on-demand insulin release from reduced graphene oxide modified hydrogels. Journal of Controlled Release, 2017, 246, 164-173.	9.9	70
113	Magnetic Fe3O4@V2O5/rGO nanocomposite as a recyclable photocatalyst for dye molecules degradation under direct sunlight irradiation. Chemosphere, 2018, 191, 503-513.	8.2	70
114	Highly improved photoreduction of carbon dioxide to methanol using cobalt phthalocyanine grafted to graphitic carbon nitride as photocatalyst under visible light irradiation. Journal of Colloid and Interface Science, 2019, 543, 201-213.	9.4	70
115	Biomolecule and Nanoparticle Transfer on Patterned and Heterogeneously Wetted Superhydrophobic Silicon Nanowire Surfaces. Langmuir, 2008, 24, 1670-1672.	3.5	69
116	Nanodiamond particles/reduced graphene oxide composites as efficient supercapacitor electrodes. Carbon, 2014, 68, 175-184.	10.3	69
117	Hexamolybdenum clusters supported on graphene oxide: Visible-light induced photocatalytic reduction of carbon dioxide into methanol. Carbon, 2015, 94, 91-100.	10.3	69
118	N-doped porous reduced graphene oxide as an efficient electrode material for high performance flexible solid-state supercapacitor. Applied Materials Today, 2017, 8, 141-149.	4.3	69
119	Preparation and Characterization of Thin Films of SiOxon Gold Substrates for Surface Plasmon Resonance Studies. Langmuir, 2006, 22, 1660-1663.	3.5	68
120	Simultaneous electrochemical detection of tryptophan and tyrosine using boron-doped diamond and diamond nanowire electrodes. Electrochemistry Communications, 2013, 35, 84-87.	4.7	67
121	Preparation of silver nanoparticles/polydopamine functionalized polyacrylonitrile fiber paper and its catalytic activity for the reduction 4-nitrophenol. Applied Surface Science, 2017, 411, 163-169.	6.1	67
122	Facile synthesis of carbon-ZnO nanocomposite with enhanced visible light photocatalytic performance. Applied Surface Science, 2017, 400, 461-470.	6.1	67
123	Label-Free Detection of Lectins on Carbohydrate-Modified Boron-Doped Diamond Surfaces. Analytical Chemistry, 2010, 82, 8203-8210.	6.5	66
124	Cumulative effect of zinc oxide and titanium oxide nanoparticles on growth and chlorophyll a content of Picochlorum sp Environmental Science and Pollution Research, 2016, 23, 2821-2830.	5.3	66
125	Modification of Porous Silicon Surfaces with Activated Ester Monolayers. Langmuir, 2002, 18, 6081-6087.	3.5	65
126	Contact angle hysteresis origins: Investigation on super-omniphobic surfaces. Soft Matter, 2011, 7, 9380.	2.7	65

#	Article	IF	CITATIONS
127	Photocatalytic activity of silicon nanowires under UV and visible light irradiation. Chemical Communications, 2011, 47, 991-993.	4.1	65
128	Graphene-Coated Surface Plasmon Resonance Interfaces for Studying the Interactions between Bacteria and Surfaces. ACS Applied Materials & amp; Interfaces, 2014, 6, 5422-5431.	8.0	65
129	Hydrothermal synthesis, phase structure, optical and photocatalytic properties of Zn2SnO4 nanoparticles. Journal of Colloid and Interface Science, 2015, 457, 360-369.	9.4	65
130	Efficient detoxification of Cr(VI)-containing effluents by sequential adsorption and reduction using a novel cysteine-doped PANi@faujasite composite: Experimental study supported by advanced statistical physics prediction. Journal of Hazardous Materials, 2022, 422, 126857.	12.4	65
131	Sensitive sugar detection using 4-aminophenylboronic acid modified graphene. Biosensors and Bioelectronics, 2013, 50, 331-337.	10.1	64
132	Efficient oil/water separation by superhydrophobic CuxS coated on copper mesh. Separation and Purification Technology, 2019, 215, 573-581.	7.9	64
133	A facile preparation of CuS-BSA nanocomposite as enzyme mimics: Application for selective and sensitive sensing of Cr(VI) ions. Sensors and Actuators B: Chemical, 2019, 294, 253-262.	7.8	64
134	"Reagentless―Micropatterning of Organics on Silicon Surfaces: Control of Hydrophobic/Hydrophilic Domains1. Journal of the American Chemical Society, 2001, 123, 1535-1536.	13.7	63
135	Transdermal skin patch based on reduced graphene oxide: A new approach for photothermal triggered permeation of ondansetron across porcine skin. Journal of Controlled Release, 2017, 245, 137-146.	9.9	63
136	Functionalization of Reduced Graphene Oxide via Thiol–Maleimide "Click―Chemistry: Facile Fabrication of Targeted Drug Delivery Vehicles. ACS Applied Materials & Interfaces, 2017, 9, 34194-34203.	8.0	63
137	CuS Decorated Functionalized Reduced Graphene Oxide: A Dual Responsive Nanozyme for Selective Detection and Photoreduction of Cr(VI) in an Aqueous Medium. ACS Sustainable Chemistry and Engineering, 2019, 7, 16131-16143.	6.7	63
138	Nanomaterials for transdermal drug delivery: beyond the state of the art of liposomal structures. Journal of Materials Chemistry B, 2017, 5, 8653-8675.	5.8	62
139	Reduced graphene oxide–based field effect transistors for the detection of E7 protein of human papillomavirus in saliva. Analytical and Bioanalytical Chemistry, 2021, 413, 779-787.	3.7	62
140	Photoluminescence stabilization of anodically-oxidized porous silicon layers by chemical functionalization. Applied Physics Letters, 2002, 81, 601-603.	3.3	61
141	Non-enzymatic glucose sensing on long and short diamond nanowire electrodes. Electrochemistry Communications, 2013, 34, 286-290.	4.7	60
142	Localized surface plasmon-enhanced fluorescence spectroscopy for highly-sensitive real-time detection of DNA hybridization. Biosensors and Bioelectronics, 2010, 25, 2579-2585.	10.1	59
143	Preparation of graphene/tetrathiafulvalene nanocomposite switchable surfaces. Chemical Communications, 2012, 48, 1221-1223.	4.1	59
144	Antibacterial Applications of Nanodiamonds. International Journal of Environmental Research and Public Health, 2016, 13, 413.	2.6	59

#	Article	IF	CITATIONS
145	Influence of the surface termination on the electrochemical properties of boron-doped diamond (BDD) interfaces. Electrochemistry Communications, 2008, 10, 402-406.	4.7	58
146	Graphite oxide: an efficient reagent for oxidation of alcohols under sonication. Tetrahedron Letters, 2012, 53, 4962-4965.	1.4	58
147	Surface Plasmon Resonance based sensing of lysozyme in serum on Micrococcus lysodeikticus-modified graphene oxide surfaces. Biosensors and Bioelectronics, 2017, 89, 525-531.	10.1	58
148	Direct amination of hydrogen-terminated boron doped diamond surfaces. Electrochemistry Communications, 2006, 8, 1185-1190.	4.7	57
149	Comparison of different oxidation techniques on single-crystal and nanocrystalline diamond surfaces. Diamond and Related Materials, 2010, 19, 474-478.	3.9	57
150	Reduced Graphene Oxide Modified Electrodes for Sensitive Sensing of Gliadin in Food Samples. ACS Sensors, 2016, 1, 1462-1470.	7.8	57
151	Toxicity effect of graphene oxide on growth and photosynthetic pigment of the marine alga Picochlorum sp. during different growth stages. Environmental Science and Pollution Research, 2017, 24, 4144-4152.	5.3	57
152	Phytic acid-doped polyaniline nanofibers-clay mineral for efficient adsorption of copper (II) ions. Journal of Colloid and Interface Science, 2019, 553, 688-698.	9.4	57
153	Au-assisted electroless etching of silicon in aqueous HF/H2O2 solution. Applied Surface Science, 2009, 255, 6210-6216.	6.1	56
154	Approach for Plasmonic Based DNA Sensing: Amplification of the Wavelength Shift and Simultaneous Detection of the Plasmon Modes of Gold Nanostructures. Analytical Chemistry, 2013, 85, 3288-3296.	6.5	56
155	Visible Light Assisted Photocatalytic [3 + 2] Azide–Alkyne "Click―Reaction for the Synthesis of 1,4-Substituted 1,2,3-Triazoles Using a Novel Bimetallic Ru–Mn Complex. ACS Sustainable Chemistry and Engineering, 2016, 4, 69-75.	6.7	56
156	Short- and Long-Range Sensing on Gold Nanostructures, Deposited on Glass, Coated with Silicon Oxide Films of Different Thicknesses. Journal of Physical Chemistry C, 2008, 112, 8239-8243.	3.1	55
157	Reversible Electrowetting on Superhydrophobic Double-Nanotextured Surfaces. Langmuir, 2009, 25, 6551-6558.	3.5	55
158	Thiol-yne Reaction on Boron-Doped Diamond Electrodes: Application for the Electrochemical Detection of DNA–DNA Hybridization Events. Analytical Chemistry, 2012, 84, 194-200.	6.5	55
159	A novel Ru/TiO <sub>2</sub> hybrid nanocomposite catalyzed photoreduction of CO <sub>2</sub> to methanol under visible light. Nanoscale, 2015, 7, 15258-15267.	5.6	55
160	Oxidative Burst-Dependent NETosis Is Implicated in the Resolution of Necrosis-Associated Sterile Inflammation. Frontiers in Immunology, 2016, 7, 557.	4.8	55
161	Facile preparation of high density polyethylene superhydrophobic/superoleophilic coatings on glass, copper and polyurethane sponge for self-cleaning, corrosion resistance and efficient oil/water separation. Journal of Colloid and Interface Science, 2018, 525, 76-85.	9.4	55
162	Electrochemical cardiovascular platforms: Current state of the art and beyond. Biosensors and Bioelectronics, 2019, 131, 287-298.	10.1	55

#	Article	IF	CITATIONS
163	Development of a novel PANI@WO3 hybrid composite and its application as a promising adsorbent for Cr(VI) ions removal. Journal of Environmental Chemical Engineering, 2021, 9, 105885.	6.7	55
164	Water Exclusion at the Nanometer Scale Provides Long-Term Passivation of Silicon (111) Grafted with Alkyl Monolayers. Journal of Physical Chemistry B, 2006, 110, 5576-5585.	2.6	54
165	Anti-MRSA Activities of Enterocins DD28 and DD93 and Evidences on Their Role in the Inhibition of Biofilm Formation. Frontiers in Microbiology, 2016, 7, 817.	3.5	54
166	Hydrothermal preparation of MoS2/TiO2/Si nanowires composite with enhanced photocatalytic performance under visible light. Materials and Design, 2016, 109, 634-643.	7.0	54
167	Detection of folic acid protein in human serum using reduced graphene oxide electrodes modified by folic-acid. Biosensors and Bioelectronics, 2016, 75, 389-395.	10.1	54
168	Nickel oxide nanoparticles grafted on reduced graphene oxide (rGO/NiO) as efficient photocatalyst for reduction of nitroaromatics under visible light irradiation. Journal of Photochemistry and Photobiology A: Chemistry, 2017, 336, 198-207.	3.9	54
169	Electrochemical impedance spectroscopy of ZnO nanostructures. Electrochemistry Communications, 2009, 11, 945-949.	4.7	53
170	A 980 nm driven photothermal ablation of virulent and antibiotic resistant Gram-positive and Gram-negative bacteria strains using Prussian blue nanoparticles. Journal of Colloid and Interface Science, 2016, 480, 63-68.	9.4	53
171	Copper oxide supported on three-dimensional ammonia-doped porous reduced graphene oxide prepared through electrophoretic deposition for non-enzymatic glucose sensing. Electrochimica Acta, 2017, 224, 346-354.	5.2	53
172	Stability of the Gold/Silica Thin Film Interface:  Electrochemical and Surface Plasmon Resonance Studies. Langmuir, 2006, 22, 10716-10722.	3.5	52
173	Controllable growth of durable superhydrophobic coatings on a copper substrate via electrodeposition. Physical Chemistry Chemical Physics, 2015, 17, 10871-10880.	2.8	52
174	Inhibition of type 1 fimbriae-mediated Escherichia coli adhesion and biofilm formation by trimeric cluster thiomannosides conjugated to diamond nanoparticles. Nanoscale, 2015, 7, 2325-2335.	5.6	52
175	Reduced graphene oxide as an efficient support for CdS-MoS2 heterostructures for enhanced photocatalytic H2 evolution. International Journal of Hydrogen Energy, 2017, 42, 16449-16458.	7.1	52
176	Nanoscale Wettability of Self-Assembled Monolayers Investigated by Noncontact Atomic Force Microscopy. Langmuir, 2006, 22, 116-126.	3.5	51
177	Graphite oxide mediated oxidative aromatization of 1,4-dihydropyridines into pyridine derivatives. Tetrahedron Letters, 2012, 53, 2473-2475.	1.4	51
178	Glucose-Derived Porous Carbon-Coated Silicon Nanowires as Efficient Electrodes for Aqueous Micro-Supercapacitors. ACS Applied Materials & Interfaces, 2016, 8, 4298-4302.	8.0	51
179	Electrochemical investigation of gold/silica thin film interfaces for electrochemical surface plasmon resonance studies. Electrochemistry Communications, 2006, 8, 439-444.	4.7	50
180	Synthesis and Luminescence Properties of (N-Doped) ZnO Nanostructures from a Dimethylformamide Aqueous Solution. Journal of Physical Chemistry C, 2009, 113, 13643-13650.	3.1	50

#	Article	IF	CITATIONS
181	Selective Adhesion of <i>Bacillus cereus</i> Spores on Heterogeneously Wetted Silicon Nanowires. Langmuir, 2010, 26, 3479-3484.	3.5	50
182	Effect of surface roughness and chemical composition on the wetting properties of silicon-based substrates. Comptes Rendus Chimie, 2013, 16, 65-72.	0.5	50
183	Photoreduction of CO2 to methanol with hexanuclear molybdenum [Mo6Br14]2â^' cluster units under visible light irradiation. RSC Advances, 2014, 4, 10420.	3.6	50
184	Repeated photoporation with graphene quantum dots enables homogeneous labeling of live cells with extrinsic markers for fluorescence microscopy. Light: Science and Applications, 2018, 7, 47.	16.6	50
185	A simple and efficient hydrogenation of benzyl alcohols to methylene compounds using triethylsilane and a palladium catalyst. Tetrahedron Letters, 2009, 50, 5930-5932.	1.4	49
186	Bioinspired Anchorable Thiol-Reactive Polymers: Synthesis and Applications Toward Surface Functionalization of Magnetic Nanoparticles. Macromolecules, 2014, 47, 5124-5134.	4.8	49
187	Nanodiamond–PMO for two-photon PDT and drug delivery. Journal of Materials Chemistry B, 2016, 4, 5803-5808.	5.8	49
188	High-Energy Flexible Supercapacitor—Synergistic Effects of Polyhydroquinone and RuO <sub>2</sub> · <i>x</i> H <sub>2</sub> O with Microsized, Few-Layered, Self-Supportive Exfoliated-Graphite Sheets. ACS Applied Materials & Interfaces, 2019, 11, 18349-18360.	8.0	49
189	Core-shell Ni/NiO grafted cobalt (II) complex: An efficient inorganic nanocomposite for photocatalytic reduction of CO2 under visible light irradiation. Applied Surface Science, 2019, 467-468, 370-381.	6.1	49
190	Substituent Effects on the Reactivity of the Siliconâ^'Carbon Double Bond. Resonance, Inductive, and Steric Effects of Substituents at Silicon on the Reactivity of Simple 1-Methylsilenes. Journal of the American Chemical Society, 1998, 120, 9504-9512.	13.7	48
191	Thin chitosan films as a platform for SPR sensing of ferric ions. Analyst, The, 2008, 133, 673.	3.5	48
192	Distinction between surface hydroxyl and ether groups on boron-doped diamond electrodes using a chemical approach. Electrochemistry Communications, 2010, 12, 351-354.	4.7	48
193	Nanomolar Hydrogen Peroxide Detection Using Horseradish Peroxidase Covalently Linked to Undoped Nanocrystalline Diamond Surfaces. Langmuir, 2012, 28, 587-592.	3.5	48
194	Sliding Droplets on Superomniphobic Zinc Oxide Nanostructures. Langmuir, 2012, 28, 389-395.	3.5	48
195	Nitro-oxidative species in vivo biosensing: Challenges and advances with focus on peroxynitrite quantification. Biosensors and Bioelectronics, 2014, 58, 359-373.	10.1	48
196	Co <sub>2</sub> SnO <sub>4</sub> nanoparticles as a high performance catalyst for oxidative degradation of rhodamine B dye and pentachlorophenol by activation of peroxymonosulfate. Physical Chemistry Chemical Physics, 2017, 19, 6569-6578.	2.8	48
197	One-step immersion for fabrication of superhydrophobic/superoleophilic carbon felts with fire resistance: Fast separation and removal of oil from water. Chemical Engineering Journal, 2018, 331, 372-382.	12.7	48
198	Toxicity Effect of Silver Nanoparticles on Photosynthetic Pigment Content, Growth, ROS Production and Ultrastructural Changes of Microalgae Chlorella vulgaris. Nanomaterials, 2019, 9, 914.	4.1	48

#	Article	IF	CITATIONS
199	Functionalization of Glassy Carbon with Diazonium Salts in Ionic Liquids. Langmuir, 2008, 24, 6327-6333.	3.5	47
200	Mesoporous silica nanoparticles in recent photodynamic therapy applications. Photochemical and Photobiological Sciences, 2018, 17, 1651-1674.	2.9	47
201	Simultaneous photocatalytic Cr(VI) reduction and phenol degradation over copper sulphide-reduced graphene oxide nanocomposite under visible light irradiation: Performance and reaction mechanism. Chemosphere, 2021, 268, 128798.	8.2	47
202	Structural and optical characterization of p-type highly Fe-doped SnO2 thin films and tunneling transport on SnO2:Fe/p-Si heterojunction. Applied Surface Science, 2018, 434, 879-890.	6.1	46
203	Hypericin-loaded lipid nanocapsules for photodynamic cancer therapy in vitro. Nanoscale, 2013, 5, 10562.	5.6	45
204	Convenient and Efficient One-Pot Method for the Synthesis of 2-Amino-tetrahydro-4 <i>H</i> -chromenes and 2-Amino-4 <i>H</i> -benzo[ <i>h</i> ]-chromenes Using Catalytic Amount of Amino-Functionalized MCM-41 in Aqueous Media. Synthetic Communications, 2013, 43, 1499-1507.	2.1	45
205	Preparation of superhydrophobic and oleophobic diamond nanograss array. Journal of Materials Chemistry, 2010, 20, 10671.	6.7	44
206	Preparation of a Responsive Carbohydrate-Coated Biointerface Based on Graphene/Azido-Terminated Tetrathiafulvalene Nanohybrid Material. ACS Applied Materials & Interfaces, 2012, 4, 5386-5393.	8.0	44
207	Graphite oxide: a simple and efficient solid acid catalyst for the ring-opening of epoxides by alcohols. Tetrahedron Letters, 2014, 55, 6694-6697.	1.4	44
208	Enhancing LSPR Sensitivity of Au Gratings through Graphene Coupling to Au Film. Plasmonics, 2014, 9, 507-512.	3.4	44
209	Antimicrobial activity of menthol modified nanodiamond particles. Diamond and Related Materials, 2015, 57, 2-8.	3.9	44
210	Electrochemically triggered release of drugs. European Polymer Journal, 2016, 83, 467-477.	5.4	44
211	Effect of high Fe doping on Raman modes and optical properties of hydrothermally prepared SnO 2 nanoparticles. Materials Science in Semiconductor Processing, 2018, 77, 31-39.	4.0	44
212	Short- and Long-Range Sensing Using Plasmonic Nanostrucures: Experimental and Theoretical Studies. Journal of Physical Chemistry C, 2009, 113, 15921-15927.	3.1	43
213	Aptamer-Based Electrochemical Sensing of Lysozyme. Chemosensors, 2016, 4, 10.	3.6	43
214	Preparation and characterization of Ni-doped ZnO–SnO2 nanocomposites: Application in photocatalysis. Superlattices and Microstructures, 2016, 91, 225-237.	3.1	43
215	Seed-mediated electrochemical growth of gold nanostructures on indium tin oxide thin films. Electrochimica Acta, 2008, 53, 7838-7844.	5.2	42
216	Clicking ferrocene groups to boron-doped diamond electrodes. Chemical Communications, 2009, , 2753.	4.1	42

#	Article	IF	CITATIONS
217	Investigation of Silicon-Based Nanostructure Morphology and Chemical Termination on Laser Desorption Ionization Mass Spectrometry Performance. Analytical Chemistry, 2012, 84, 10637-10644.	6.5	42
218	Peroxynitrite activity of hemin-functionalized reduced graphene oxide. Analyst, The, 2013, 138, 4345.	3.5	42
219	Flexible Nanoholey Patches for Antibiotic-Free Treatments of Skin Infections. ACS Applied Materials & Interfaces, 2017, 9, 36665-36674.	8.0	42
220	Au Ni alloy nanoparticles supported on reduced graphene oxide as highly efficient electrocatalysts for hydrogen evolution and oxygen reduction reactions. International Journal of Hydrogen Energy, 2018, 43, 1424-1438.	7.1	42
221	Fabrication of superhydrophobic/superoleophilic functionalized reduced graphene oxide/polydopamine/PFDT membrane for efficient oil/water separation. Separation and Purification Technology, 2020, 236, 116240.	7.9	42
222	The versatile behavior of the PdCl2/Et3SiH system. Conversion of alcohols to the corresponding halides and alkanes. Journal of Organometallic Chemistry, 1998, 554, 135-137.	1.8	41
223	Hidden Electrochemistry in the Thermal Grafting of Silicon Surfaces from Grignard Reagents. Langmuir, 2004, 20, 6359-6364.	3.5	41
224	Surface-assisted laser desorption–ionization mass spectrometry on titanium dioxide (TiO2) nanotube layers. Analyst, The, 2012, 137, 3058.	3.5	41
225	Electro-(de)wetting on Superhydrophobic Surfaces. Langmuir, 2013, 29, 13346-13351.	3.5	41
226	Diamond Nanowires: A Novel Platform for Electrochemistry and Matrix-Free Mass Spectrometry. Sensors, 2015, 15, 12573-12593.	3.8	41
227	Reduction of Cr(VI) to Cr(III) using silicon nanowire arrays under visible light irradiation. Journal of Hazardous Materials, 2016, 304, 441-447.	12.4	41
228	Design and preparation of core-shell structured magnetic graphene oxide@MIL-101(Fe): Photocatalysis under shell to remove diazinon and atrazine pesticides. Solar Energy, 2020, 208, 990-1000.	6.1	41
229	Facile interfacial electron transfer through n-alkyl monolayers formed on silicon (111) surfaces. Electrochemistry Communications, 2000, 2, 562-566.	4.7	40
230	Selective detection of hexachromium ions by localized surface plasmon resonance measurements using gold nanoparticles/chitosan composite interfaces. Analyst, The, 2009, 134, 881.	3.5	40
231	Non-Enzymatic Glucose Sensing Using Carbon Quantum Dots Decorated with Copper Oxide Nanoparticles. Sensors, 2016, 16, 1720.	3.8	40
232	Advancements on the molecular design of nanoantibiotics: current level of development and future challenges. Molecular Systems Design and Engineering, 2017, 2, 349-369.	3.4	40
233	Efficient reduction of Cr(VI) under visible light irradiation using CuS nanostructures. Arabian Journal of Chemistry, 2019, 12, 215-224.	4.9	40
234	Electrochemical impedance spectroscopy and surface plasmon resonance studies of DNA hybridization on gold/SiOx interfaces. Analyst, The, 2008, 133, 1097.	3.5	39

#	Article	IF	CITATIONS
235	From micro to nano reentrant structures: hysteresis on superomniphobic surfaces. Colloid and Polymer Science, 2013, 291, 409-415.	2.1	39
236	Dependence between the Refractive-Index Sensitivity of Metallic Nanoparticles and the Spectral Position of Their Localized Surface Plasmon Band: A Numerical and Analytical Study. Journal of Physical Chemistry C, 2015, 119, 28551-28559.	3.1	39
237	Graphene Oxide Supported Molybdenum Cluster: First Heterogenized Homogeneous Catalyst for the Synthesis of Dimethylcarbonate from CO 2 and Methanol. Chemistry - A European Journal, 2015, 21, 3488-3494.	3.3	39
238	Phenyl-grafted carbon nitride semiconductor for photocatalytic CO <sub>2</sub> -reduction and rapid degradation of organic dyes. Catalysis Science and Technology, 2019, 9, 822-832.	4.1	39
239	Graphene oxide effects in early ontogenetic stages of Triticum aestivum L. seedlings. Ecotoxicology and Environmental Safety, 2019, 181, 345-352.	6.0	39
240	Graphene-modified electrodes for sensing doxorubicin hydrochloride in human plasma. Analytical and Bioanalytical Chemistry, 2019, 411, 1509-1516.	3.7	39
241	CoS <sub>2</sub> Nanoparticles Supported on rGO, g-C <sub>3</sub> N <sub>4</sub> , BCN, MoS <sub>2</sub> , and WS <sub>2</sub> Two-Dimensional Nanosheets with Excellent Electrocatalytic Performance for Overall Water Splitting: Electrochemical Studies and DFT Calculations. ACS Applied Energy Materials, 2021, 4, 1269-1285.	5.1	39
242	Effectiveness of a novel polyaniline@Fe-ZSM-5 hybrid composite for Orange G dye removal from aqueous media: Experimental study and advanced statistical physics insights. Chemosphere, 2022, 295, 133786.	8.2	39
243	Peptide Immobilization on Amine-Terminated Boron-Doped Diamond Surfaces. Langmuir, 2007, 23, 4494-4497.	3.5	38
244	Effect of magnetic iron oxide (Fe3O4) nanoparticles on the growth and photosynthetic pigment content of Picochlorum sp Environmental Science and Pollution Research, 2015, 22, 11728-11739.	5.3	38
245	Passivated Luminescent Porous Silicon. Journal of the Electrochemical Society, 2001, 148, H91.	2.9	37
246	HREELS Investigation of the Surfaces of Nanocrystalline Diamond Films Oxidized by Different Processes. Langmuir, 2010, 26, 18798-18805.	3.5	37
247	Sensitivity of Plasmonic Nanostructures Coated with Thin Oxide Films for Refractive Index Sensing: Experimental and Theoretical Investigations. Journal of Physical Chemistry C, 2010, 114, 11769-11775.	3.1	37
248	Stacking Faults-Induced Quenching of the UV Luminescence in ZnO. Journal of Physical Chemistry Letters, 2010, 1, 3033-3038.	4.6	37
249	Surface Plasmon Resonance on Gold and Silver Films Coated with Thin Layers of Amorphous Siliconâ^'Carbon Alloys. Langmuir, 2010, 26, 6058-6065.	3.5	37
250	Investigation of the corrosion behavior of carbon steel coated with fluoropolymer thin films. Surface and Coatings Technology, 2011, 205, 4011-4017.	4.8	37
251	Voltammetric detection of l-dopa and carbidopa on graphene modified glassy carbon interfaces. Bioelectrochemistry, 2013, 93, 15-22.	4.6	37
252	Iron addition induced tunable band gap and tetravalent Fe ion in hydrothermally prepared SnO2 nanocrystals: Application in photocatalysis. Materials Research Bulletin, 2016, 83, 481-490.	5.2	37

#	Article	IF	CITATIONS
253	Controlled fabrication of NiO/ZnO superhydrophobic surface on zinc substrate with corrosion and abrasion resistance. Journal of Alloys and Compounds, 2017, 723, 225-236.	5.5	37
254	Effect of cobalt addition on the corrosion behavior of near equiatomic NiTi shape memory alloy in normal saline solution: electrochemical and XPS studies. RSC Advances, 2018, 8, 19289-19300.	3.6	37
255	Functionalized MoS2/polyurethane sponge: An efficient scavenger for oil in water. Separation and Purification Technology, 2020, 238, 116420.	7.9	37
256	5,10-dihydro-silanthrene as a reagent for the Barton-McCombie reaction. Tetrahedron Letters, 1995, 36, 3897-3900.	1.4	36
257	Palladium-catalyzed reduction of olefins with triethylsilane. Tetrahedron Letters, 2003, 44, 4579-4580.	1.4	36
258	Thiol–Yne Click Reactions on Alkynyl–Dopamineâ€Modified Reduced Graphene Oxide. Chemistry - A European Journal, 2013, 19, 8673-8678.	3.3	36
259	Cathodic activation of titanium-supported gold nanoparticles: An efficient and stable electrocatalyst for the hydrogen evolution reaction. International Journal of Hydrogen Energy, 2016, 41, 6326-6341.	7.1	36
260	Electrochemically stimulated drug release from flexible electrodes coated electrophoretically with doxorubicin loaded reduced graphene oxide. Chemical Communications, 2017, 53, 4022-4025.	4.1	36
261	Gold nanoparticles coated silicon nanowires for efficient catalytic and photocatalytic applications. Materials Science in Semiconductor Processing, 2018, 75, 206-213.	4.0	36
262	Highly efficient conversion of the nitroarenes to amines at the interface of a ternary hybrid containing silver nanoparticles doped reduced graphene oxide/ graphitic carbon nitride under visible light. Journal of Hazardous Materials, 2020, 387, 121700.	12.4	36
263	Microwave Effects on Chemical Functionalization of Hydrogen-Terminated Porous Silicon Nanostructures. Journal of Physical Chemistry C, 2008, 112, 16622-16628.	3.1	35
264	Growth of Si nanowires on micropillars for the study of their dopant distribution by atom probe tomography. Journal of Vacuum Science & Technology B, 2008, 26, 1960-1963.	1.3	35
265	One-step synthesis of Au nanoparticle–graphene composites using tyrosine: electrocatalytic and catalytic properties. New Journal of Chemistry, 2016, 40, 5473-5482.	2.8	35
266	Enterocin B3A-B3B produced by LAB collected from infant faeces: potential utilization in the food industry for Listeria monocytogenes biofilm management. Antonie Van Leeuwenhoek, 2017, 110, 205-219.	1.7	35
267	Hydrogen adsorption properties of Ag decorated TiO2 nanomaterials. International Journal of Hydrogen Energy, 2018, 43, 2861-2868.	7.1	35
268	Achieving on chip micro-supercapacitors based on CrN deposited by bipolar magnetron sputtering at glancing angle. Electrochimica Acta, 2019, 324, 134890.	5.2	35
269	Heterostructures of mesoporous TiO2 and SnO2 nanocatalyst for improved electrochemical oxidation ability of vitamin B6 in pharmaceutical tablets. Journal of Colloid and Interface Science, 2019, 542, 45-53.	9.4	35
270	Dual-Ligand Fe-Metal Organic Framework Based Robust High Capacity Li Ion Battery Anode and Its Use in a Flexible Battery Format for Electro-Thermal Heating. ACS Applied Energy Materials, 2019, 2, 4450-4457.	5.1	35

#	Article	IF	CITATIONS
271	ZnO/Carbon nanowalls shell/core nanostructures as electrodes for supercapacitors. Applied Surface Science, 2019, 481, 926-932.	6.1	35
272	Extraction of Cellulose Nanocrystals with Structure I and II and Their Applications for Reduction of Graphene Oxide and Nanocomposite Elaboration. Waste and Biomass Valorization, 2019, 10, 1913-1927.	3.4	35
273	Colorimetric sensing of dopamine in beef meat using copper sulfide encapsulated within bovine serum albumin functionalized with copper phosphate (CuS-BSA-Cu3(PO4)2) nanoparticles. Journal of Colloid and Interface Science, 2021, 582, 732-740.	9.4	35
274	A novel and efficient method for double bond isomerization. Journal of Organometallic Chemistry, 2003, 678, 1-4.	1.8	34
275	Raman Imaging and Kelvin Probe Microscopy for the Examination of the Heterogeneity of Doping in Polycrystalline Boron-Doped Diamond Electrodes. Journal of Physical Chemistry B, 2006, 110, 23888-23897.	2.6	34
276	Polarization Modulation Infrared Reflection Absorption Spectroscopy Investigations of Thin Silica Films Deposited on Gold. 2. Structural Analysis of a 1,2-Dimyristoyl- <i>sn</i> -glycero-3-phosphocholine Bilayer. Langmuir, 2008, 24, 3922-3929.	3.5	34
277	Preparation and electrochemical behaviour of PPy–CdS composite films. Journal of Electroanalytical Chemistry, 2011, 650, 176-181.	3.8	34
278	Reduced Graphene Oxide Nanosheets Decorated with Au Nanoparticles as an Effective Bactericide: Investigation of Biocompatibility and Leakage of Sugars and Proteins. ChemPlusChem, 2014, 79, 1774-1784.	2.8	34
279	Carbohydrate–Lectin Interaction on Graphene-Coated Surface Plasmon Resonance (SPR) Interfaces. Plasmonics, 2014, 9, 677-683.	3.4	34
280	Electrophoretic Deposition of Carbon Nanofibers/Co(OH) <sub>2</sub> Nanocomposites: Application for Nonâ€Enzymatic Glucose Sensing. Electroanalysis, 2016, 28, 119-125.	2.9	34
281	Ultrasmall CuS-BSA-Cu3(PO4)2 nanozyme for highly efficient colorimetric sensing of H2O2 and glucose in contact lens care solutions and human serum. Analytica Chimica Acta, 2020, 1109, 78-89.	5.4	34
282	<i>In Situ</i> Synthesis of Co <sub>3</sub> O <sub>4</sub> /CoFe <sub>2</sub> O <sub>4</sub> Derived from a Metal–Organic Framework on Nickel Foam: High-Performance Electrocatalyst for Water Oxidation. ACS Applied Energy Materials, 2021, 4, 2951-2959.	5.1	34
283	Substituent Effects on the Reactivity of the Siliconâ^Carbon Double Bond. Substituted 1,1-Dimethylsilenes from Far-UV Laser Flash Photolysis of α-Silylketenes and (Trimethylsilyl)diazomethane. Journal of the American Chemical Society, 1999, 121, 4744-4753.	13.7	33
284	Preparation and Characterization of Silver Substrates Coated with Antimony-Doped SnO <sub>2</sub> Thin Films for Surface Plasmon Resonance Studies. Langmuir, 2009, 25, 8036-8041.	3.5	33
285	Development and Characterization of a Diamond-Based Localized Surface Plasmon Resonance Interface. Journal of Physical Chemistry C, 2010, 114, 3346-3353.	3.1	33
286	Surface Plasmon-Enhanced Fluorescence Spectroscopy on Silver Based SPR Substrates. Journal of Physical Chemistry C, 2010, 114, 22582-22589.	3.1	33
287	Electrowetting and droplet impalement experiments on superhydrophobic multiscale structures. Faraday Discussions, 2010, 146, 125.	3.2	33
288	Insulin loaded iron magnetic nanoparticle–graphene oxide composites: synthesis, characterization and application for in vivo delivery of insulin. RSC Advances, 2014, 4, 865-875.	3.6	33

#	Article	IF	CITATIONS
289	Selective Antimicrobial and Antibiofilm Disrupting Properties of Functionalized Diamond Nanoparticles Against <i>Escherichia coli</i> and <i>Staphylococcus aureus</i> . Particle and Particle Systems Characterization, 2015, 32, 822-830.	2.3	33
290	Nanodiamonds for bioapplications, recent developments. Journal of Materials Chemistry B, 2020, 8, 10878-10896.	5.8	33
291	High performance flexible hybrid supercapacitors based on nickel hydroxide deposited on copper oxide supported by copper foam for a sunlight-powered rechargeable energy storage system. Journal of Colloid and Interface Science, 2020, 579, 520-530.	9.4	33
292	Colorimetric assay for the detection of dopamine using bismuth ferrite oxide (Bi2Fe4O9) nanoparticles as an efficient peroxidase-mimic nanozyme. Journal of Colloid and Interface Science, 2022, 613, 384-395.	9.4	33
293	Second Harmonic Generation at Chemically Modified Si(111) Surfacesâ€. Journal of Physical Chemistry B, 2000, 104, 7668-7676.	2.6	32
294	PM IRRAS Investigation of Thin Silica Films Deposited on Gold. Part 1. Theory and Proof of Concept. Langmuir, 2007, 23, 9303-9309.	3.5	32
295	Molecular monolayers on silicon as substrates for biosensors. Bioelectrochemistry, 2010, 80, 17-25.	4.6	32
296	Laser desorption ionization mass spectrometry of protein tryptic digests on nanostructured silicon plates. Journal of Proteomics, 2012, 75, 1973-1990.	2.4	32
297	Acoustic Tracking of Cassie to Wenzel Wetting Transitions. Langmuir, 2013, 29, 13129-13134.	3.5	32
298	Comparison of photo- and Cu( <scp>i</scp> )-catalyzed "click―chemistries for the formation of carbohydrate SPR interfaces. Analyst, The, 2013, 138, 805-812.	3.5	32
299	Carbon nanowalls: a new versatile graphene based interface for the laser desorption/ionization-mass spectrometry detection of small compounds in real samples. Nanoscale, 2017, 9, 9701-9715.	5.6	32
300	Self-template synthesis of ZnS/Ni3S2 as advanced electrode material for hybrid supercapacitors. Electrochimica Acta, 2019, 328, 135065.	5.2	32
301	Colorimetric detection of chromium (VI) ion using poly(N-phenylglycine) nanoparticles acting as a peroxidase mimetic catalyst. Talanta, 2021, 226, 122082.	5.5	32
302	Facile Synthesis of Bimetal Nickel Cobalt Phosphate Nanostructures for High-Performance Hybrid Supercapacitors. Journal of Alloys and Compounds, 2022, 893, 162340.	5.5	32
303	Brillouin spectroscopy of acoustic modes in porous silicon films. Physical Review B, 2002, 65, .	3.2	31
304	A mild and efficient palladium–triethylsilane system for reduction of olefins and carbon–carbon double bond isomerization. Applied Organometallic Chemistry, 2006, 20, 214-219.	3.5	31
305	Dielectric coated plasmonic interfaces: their interest for sensitive sensing of analyte-ligand interactions. Reviews in Analytical Chemistry, 2012, 31, .	3.2	31
306	Nanometal plasmonpolaritons. Surface Science Reports, 2013, 68, 1-67.	7.2	31

#	Article	IF	CITATIONS
307	Electrophoretic Approach for the Simultaneous Deposition and Functionalization of Reduced Graphene Oxide Nanosheets with Diazonium Compounds: Application for Lysozyme Sensing in Serum. ACS Applied Materials & Interfaces, 2017, 9, 12823-12831.	8.0	31
308	Efficient capture and photothermal ablation of planktonic bacteria and biofilms using reduced graphene oxide–polyethyleneimine flexible nanoheaters. Journal of Materials Chemistry B, 2019, 7, 2771-2781.	5.8	31
309	Photochemical Immobilization of Proteins and Peptides on Benzophenone-Terminated Boron-Doped Diamond Surfaces. Langmuir, 2010, 26, 1075-1080.	3.5	30
310	Plasmonic Nanoparticles Array for High-Sensitivity Sensing: A Theoretical Investigation. Journal of Physical Chemistry C, 2012, 116, 17819-17827.	3.1	30
311	Micro-and nanostructured silicon-based superomniphobic surfaces. Journal of Colloid and Interface Science, 2014, 416, 280-288.	9.4	30
312	Environmentally Friendly Reduction of Graphene Oxide Using Tyrosine for Nonenzymatic Amperometric H <sub>2</sub> O <sub>2</sub> Detection. Electroanalysis, 2014, 26, 156-163.	2.9	30
313	Carbohydrate Microarray for the Detection of Glycan–Protein Interactions Using Metal-Enhanced Fluorescence. Analytical Chemistry, 2015, 87, 3721-3728.	6.5	30
314	Toward Multifunctional "Clickable―Diamond Nanoparticles. Langmuir, 2015, 31, 3926-3933.	3.5	30
315	Ultrasound assisted direct oxidative esterification of aldehydes and alcohols using graphite oxide and Oxone. Ultrasonics Sonochemistry, 2015, 22, 359-364.	8.2	30
316	Controlled modification of electrochemical microsystems with polyethylenimine/reduced graphene oxide using electrophoretic deposition: Sensing of dopamine levels in meat samples. Talanta, 2018, 178, 432-440.	5.5	30
317	Near-infrared light activatable hydrogels for metformin delivery. Nanoscale, 2019, 11, 15810-15820.	5.6	30
318	High performance silicon nanowires/ruthenium nanoparticles micro-supercapacitors. Electrochimica Acta, 2019, 311, 150-159.	5.2	30
319	Aluminum oxide nanowires as safe and effective adjuvants for next-generation vaccines. Materials Today, 2019, 22, 58-66.	14.2	30
320	Preparation of superhydrophobic/superoleophilic copper coated titanium mesh with excellent ice-phobic and water-oil separation performance. Applied Surface Science, 2019, 476, 353-362.	6.1	30
321	Electrothermal patches driving the transdermal delivery of insulin. Nanoscale Horizons, 2020, 5, 663-670.	8.0	30
322	Electron beam-induced modification of organic monolayers on Si(111) surfaces used for selective electrodeposition. Electrochemistry Communications, 2004, 6, 153-157.	4.7	29
323	Influence of the Surface Termination of Boron-Doped Diamond Electrodes on Oxygen Reduction in Basic Medium. Electrochemical and Solid-State Letters, 2007, 10, G43.	2.2	29
324	Covalent linking of peptides onto oxygen-terminated boron-doped diamond surfaces. Diamond and Related Materials, 2007, 16, 892-898.	3.9	29

#	Article	IF	CITATIONS
325	Cell micropatterning on superhydrophobic diamond nanowires. Acta Biomaterialia, 2013, 9, 4585-4591.	8.3	29
326	Palladium nanoparticles supported on reduced graphene oxide as an efficient catalyst for the reduction of benzyl alcohol compounds. Catalysis Communications, 2015, 69, 97-103.	3.3	29
327	Reduced graphene oxide nanosheets decorated with AuPd bimetallic nanoparticles: a multifunctional material for photothermal therapy of cancer cells. Journal of Materials Chemistry B, 2015, 3, 8366-8374.	5.8	29
328	Influence of adsorption parameters of basic red dye 46 by the rough and treated Algerian natural phosphates. Journal of Industrial and Engineering Chemistry, 2015, 25, 229-238.	5.8	29
329	Preparation of mussel-inspired perfluorinated polydopamine film on brass substrates: Superhydrophobic and anti-corrosion application. Progress in Organic Coatings, 2018, 125, 109-118.	3.9	29
330	Entrapment of uropathogenic E. coli cells into ultra-thin sol-gel matrices on gold thin films: A low cost alternative for impedimetric bacteria sensing. Biosensors and Bioelectronics, 2019, 124-125, 161-166.	10.1	29
331	Pd nanoparticles supported on reduced graphene oxide as an effective and reusable heterogeneous catalyst for the Mizoroki–Heck coupling reaction. Applied Organometallic Chemistry, 2020, 34, e5524.	3.5	29
332	A mask-based diagnostic platform for point-of-care screening of Covid-19. Biosensors and Bioelectronics, 2021, 192, 113486.	10.1	29
333	Oxone/iron(II) sulfate/graphite oxide as a highly effective system for oxidation of alcohols under ultrasonic irradiation. Tetrahedron Letters, 2014, 55, 342-345.	1.4	28
334	Ultrasound-assisted direct oxidative amidation of benzyl alcohols catalyzed by graphite oxide. Ultrasonics Sonochemistry, 2016, 32, 37-43.	8.2	28
335	Robust superhydrophobic polyurethane sponge functionalized with perfluorinated graphene oxide for efficient immiscible oil/water mixture, stable emulsion separation and crude oil dehydration. Science China Technological Sciences, 2019, 62, 1585-1595.	4.0	28
336	High performance of phytic acid-functionalized spherical poly-phenylglycine particles for removal of heavy metal ions. Applied Surface Science, 2020, 518, 146206.	6.1	28
337	The impact of chemical engineering and technological advances on managing diabetes: present and future concepts. Chemical Society Reviews, 2021, 50, 2102-2146.	38.1	28
338	"Clicking―Thiophene on Diamond Interfaces. Preparation of a Conducting Polythiophene/Diamond Hybrid Material. Journal of Physical Chemistry C, 2009, 113, 17082-17086.	3.1	27
339	Investigation of the corrosion protection of SiOx-like oxide films deposited by plasma-enhanced chemical vapor deposition onto carbon steel. Electrochimica Acta, 2010, 55, 8921-8927.	5.2	27
340	Combed Single DNA Molecules Imaged by Secondary Ion Mass Spectrometry. Analytical Chemistry, 2011, 83, 6940-6947.	6.5	27
341	Unprecedented inhibition of glycosidase-catalyzed substrate hydrolysis by nanodiamond-grafted O-glycosides. RSC Advances, 2015, 5, 100568-100578.	3.6	27
342	Effect of incubation duration, growth temperature, and abiotic surface type on cell surface properties, adhesion and pathogenicity of biofilm-detached Staphylococcus aureus cells. AMB Express, 2017, 7, 191.	3.0	27

#	Article	IF	CITATIONS
343	An â€~on-demand' photothermal antibiotic release cryogel patch: evaluation of efficacy on an <i>ex vivo</i> model for skin wound infection. Biomaterials Science, 2020, 8, 5911-5919.	5.4	27
344	NiMnCr layered double hydroxide-carbon spheres modified Ni foam: An efficient positive electrode for hybrid supercapacitors. Chemical Engineering Journal, 2020, 396, 125370.	12.7	27
345	Ultra-sensitive and fast optical detection of the spike protein of the SARS-CoV-2 using AgNPs/SiNWs nanohybrid based sensors. Surfaces and Interfaces, 2021, 27, 101454.	3.0	27
346	Palladium-catalyzed protection of alcohols and cleavage of triethylsilyl ethers. Journal of Organometallic Chemistry, 2005, 690, 2372-2375.	1.8	26
347	Controlled growth of silicon nanowires on silicon surfaces. Journal of Electroceramics, 2006, 16, 15-21.	2.0	26
348	Palladium catalyzed mild reduction of $\hat{l}_{\pm}, \hat{l}^2$ -unsaturated compounds by triethylsilane. Journal of Organometallic Chemistry, 2007, 692, 5113-5116.	1.8	26
349	Synthesis and photoluminescence properties of silicon nanowires treated by high-pressure water vapor annealing. Physica Status Solidi (A) Applications and Materials Science, 2007, 204, 1302-1306.	1.8	26
350	Efficient method for the reduction of carbonyl compounds by triethylsilane catalyzed by PdCl2. Journal of Organometallic Chemistry, 2008, 693, 3567-3570.	1.8	26
351	Amorphous silicon–carbon alloys for efficient localized surface plasmon resonance sensing. Biosensors and Bioelectronics, 2010, 25, 1199-1203.	10.1	26
352	Amplified plasmonic detection of DNA hybridization using doxorubicin-capped gold particles. Analyst, The, 2014, 139, 157-164.	3.5	26
353	Electrochemically triggered release of human insulin from an insulin-impregnated reduced graphene oxide modified electrode. Chemical Communications, 2015, 51, 14167-14170.	4.1	26
354	MoS2/reduced graphene oxide nanocomposite for sensitive sensing of cysteamine in presence of uric acid in human plasma. Materials Science and Engineering C, 2017, 73, 627-632.	7.3	26
355	Fe-doped SnO2 decorated reduced graphene oxide nanocomposite with enhanced visible light photocatalytic activity. Journal of Photochemistry and Photobiology A: Chemistry, 2018, 367, 145-155.	3.9	26
356	Exploring Light-Sensitive Nanocarriers for Simultaneous Triggered Antibiotic Release and Disruption of Biofilms Upon Generation of Laser-Induced Vapor Nanobubbles. Pharmaceutics, 2019, 11, 201.	4.5	26
357	Near edge X-ray absorption fine structure spectroscopy of chemically modified porous silicon. Journal of Electron Spectroscopy and Related Phenomena, 2004, 135, 143-147.	1.7	25
358	Bovine serum albumin adsorption on passivated porous silicon layers. Canadian Journal of Chemistry, 2004, 82, 1545-1553.	1.1	25
359	Preparation of Electrochemical and Surface Plasmon Resonance Active Interfaces: Deposition of Indium Tin Oxide on Silver Thin Films. Journal of Physical Chemistry C, 2008, 112, 10883-10888.	3.1	25
360	Development of a Metal-Chelated Plasmonic Interface for the Linking of His-Peptides with a Droplet-Based Surface Plasmon Resonance Read-Off Scheme. Langmuir, 2011, 27, 5498-5505.	3.5	25

#	Article	IF	CITATIONS
361	Inhibiting protein biofouling using graphene oxide in droplet-based microfluidic microsystems. Lab on A Chip, 2012, 12, 1601.	6.0	25
362	Highly effective photodynamic inactivation of E. coli using gold nanorods/SiO <sub>2</sub> core–shell nanostructures with embedded verteporfin. Chemical Communications, 2015, 51, 16365-16368.	4.1	25
363	Boronic acid-modified lipid nanocapsules: a novel platform for the highly efficient inhibition of hepatitis C viral entry. Nanoscale, 2015, 7, 1392-1402.	5.6	25
364	Hydrothermal synthesis of ZTO/graphene nanocomposite with excellent photocatalytic activity under visible light irradiation. Journal of Colloid and Interface Science, 2016, 473, 66-74.	9.4	25
365	Solution Processable Cu(II)macrocycle for the Formation of Cu <sub>2</sub> 0 Thin Film on Indium Tin Oxide and Its Application for Water Oxidation. Journal of Physical Chemistry C, 2018, 122, 16510-16518.	3.1	25
366	Photografting and patterning of oligonucleotides on benzophenone-modified boron-doped diamond. Chemical Communications, 2007, , 2793.	4.1	24
367	Formation of aligned silicon-nanowire on silicon in aqueous HF/(AgNO3+Na2S2O8) solution. Applied Surface Science, 2008, 254, 7219-7222.	6.1	24
368	Preparation and characterization of antimony-doped SnO2 thin films on gold and silver substrates for electrochemical and surface plasmon resonance studies. Electrochemistry Communications, 2008, 10, 1041-1043.	4.7	24
369	Formation of aligned silicon nanowire on silicon by electroless etching in HF solution. Journal of Luminescence, 2009, 129, 1750-1753.	3.1	24
370	Lipid nanocapsules functionalized with polyethyleneimine for plasmid DNA and drug co-delivery and cell imaging. Nanoscale, 2014, 6, 7379.	5.6	24
371	A Prussian blue/carbon dot nanocomposite as an efficient visible light active photocatalyst for C-H activation of amines. Photochemical and Photobiological Sciences, 2016, 15, 1282-1288.	2.9	24
372	MoS2/TiO2/SiNW surface as an effective substrate for LDI-MS detection of glucose and glutathione in real samples. Talanta, 2017, 171, 101-107.	5.5	24
373	Controlled covalent functionalization of a graphene-channel of a field effect transistor as an ideal platform for (bio)sensing applications. Nanoscale Horizons, 2021, 6, 819-829.	8.0	24
374	Highly performing graphene-based field effect transistor for the differentiation between mild-moderate-severe myocardial injury. Nano Today, 2022, 43, 101391.	11.9	24
375	Second harmonic generation spectroscopy of chemically modified Si(111) surfaces. Surface Science, 2001, 488, 367-378.	1.9	23
376	Enhanced conductance of chlorine-terminated Si(111) surfaces: Formation of a two-dimensional hole gas via chemical modification. Physical Review B, 2005, 71, .	3.2	23
377	Covalent modification of boron-doped diamond electrodes with an imidazolium-based ionic liquid. Electrochimica Acta, 2010, 55, 1582-1587.	5.2	23
378	Vertical arrays of SiNWs–ZnO nanostructures as high performance electron field emitters. Journal of Materials Chemistry, 2012, 22, 22922.	6.7	23

#	Article	IF	CITATIONS
379	Affinity surface-assisted laser desorption/ionization mass spectrometry for peptide enrichment. Analyst, The, 2012, 137, 5527.	3.5	23
380	Near-Field and Far-Field Sensitivities of LSPR Sensors. Journal of Physical Chemistry C, 2015, 119, 9470-9476.	3.1	23
381	Insulin impregnated reduced graphene oxide/Ni(OH)2 thin films for electrochemical insulin release and glucose sensing. Sensors and Actuators B: Chemical, 2016, 237, 693-701.	7.8	23
382	Selective isolation and eradication of E. coli associated with urinary tract infections using anti-fimbrial modified magnetic reduced graphene oxide nanoheaters. Journal of Materials Chemistry B, 2017, 5, 8133-8142.	5.8	23
383	Cu(0) nanoparticle-decorated functionalized reduced graphene oxide sheets as artificial peroxidase enzymes: application for colorimetric detection of Cr( <scp>vi</scp> ) ions. New Journal of Chemistry, 2019, 43, 1404-1414.	2.8	23
384	Evaporation behavior of PEGylated graphene oxide nanofluid droplets on heated substrate. International Journal of Thermal Sciences, 2019, 135, 445-458.	4.9	23
385	Covalent grafting of polyaniline onto aniline-terminated porous silicon. Optical Materials, 2010, 32, 748-752.	3.6	22
386	Electrochemical grafting of poly(3â€hexylthiophene) on porous silicon for gas sensing. Surface and Interface Analysis, 2010, 42, 1041-1045.	1.8	22
387	Magnetic Co <sub>3</sub> O <sub>4</sub> /reduced graphene oxide nanocomposite as a superior heterogeneous catalyst for one-pot oxidative esterification of aldehydes to methyl esters. RSC Advances, 2015, 5, 88567-88573.	3.6	22
388	Revealing the structure and functionality of graphene oxide and reduced graphene oxide/pyrene carboxylic acid interfaces by correlative spectral and imaging analysis. Physical Chemistry Chemical Physics, 2017, 19, 16038-16046.	2.8	22
389	Graphene-based nanomaterials in innovative electrochemistry. Current Opinion in Electrochemistry, 2018, 10, 24-30.	4.8	22
390	Encapsulation of a TRPM8 Agonist, WS12, in Lipid Nanocapsules Potentiates PC3 Prostate Cancer Cell Migration Inhibition through Channel Activation. Scientific Reports, 2019, 9, 7926.	3.3	22
391	Photothermally Active Cryogel Devices for Effective Release of Antimicrobial Peptides: On-Demand Treatment of Infections. ACS Applied Materials & Interfaces, 2020, 12, 56805-56814.	8.0	22
392	Zirconocyclisation: Access to new racemic (di) phosphines. Tetrahedron Letters, 1996, 37, 3109-3112.	1.4	21
393	Chips from Chips: Application to the Study of Antibody Responses to Methylated Proteins. Journal of Proteome Research, 2010, 9, 6467-6478.	3.7	21
394	Preparation and characterization of Zonyl-coated nanodiamonds with antifouling properties. Chemical Communications, 2011, 47, 5178.	4.1	21
395	Octahedral rhenium K4[Re6S8(CN)6] and Cu(OH)2 cluster modified TiO2 for the photoreduction of CO2 under visible light irradiation. Applied Catalysis A: General, 2015, 499, 32-38.	4.3	21
396	Plasmon-Driven Electrochemical Methanol Oxidation on Gold Nanohole Electrodes. ACS Applied Materials & Interfaces, 2020, 12, 50426-50432.	8.0	21

#	Article	IF	CITATIONS
397	Heterologous Biosynthesis of Five New Class II Bacteriocins From Lactobacillus paracasei CNCM I-5369 With Antagonistic Activity Against Pathogenic Escherichia coli Strains. Frontiers in Microbiology, 2020, 11, 1198.	3.5	21
398	Aluminum based metal-organic framework integrated with reduced graphene oxide for improved supercapacitive performance. Electrochimica Acta, 2020, 353, 136609.	5.2	21
399	Purification for Carbon Nanotubes Synthesized by Flame Fragments Deposition via Hydrogen Peroxide and Acetone. Materials, 2020, 13, 2342.	2.9	21
400	Innovative transdermal delivery of insulin using gelatin methacrylate-based microneedle patches in mice and mini-pigs. Nanoscale Horizons, 2022, 7, 174-184.	8.0	21
401	Localized electropolymerization on oxidized boron-doped diamond electrodes modified with pyrrolyl units. Physical Chemistry Chemical Physics, 2006, 8, 4924.	2.8	20
402	Electrosynthesis and analysis of the electrochemical properties of a composite material: Polyaniline + titanium oxide. Thin Solid Films, 2011, 519, 3596-3602.	1.8	20
403	Diamond nanowires decorated with metallic nanoparticles: A novel electrical interface for the immobilization of histidinylated biomolecuels. Electrochimica Acta, 2013, 110, 4-8.	5.2	20
404	Graphite oxide as an efficient solid reagent for esterification reactions. Turkish Journal of Chemistry, 2014, 38, 859-864.	1.2	20
405	Quantitative Assessment of the Multivalent Protein–Carbohydrate Interactions on Silicon. Analytical Chemistry, 2014, 86, 10340-10349.	6.5	20
406	Palladium on activated carbon catalyzed reductive amination of aldehydes and ketones by triethylsilane. Applied Organometallic Chemistry, 2014, 28, 113-115.	3.5	20
407	Fabrication of superhydrophobic and highly oleophobic silicon-based surfaces via electroless etching method. Applied Surface Science, 2014, 295, 38-43.	6.1	20
408	Enhanced Ultraviolet Luminescence of ZnO Nanorods Treated by High-Pressure Water Vapor Annealing (HWA). Journal of Physical Chemistry C, 2016, 120, 4571-4580.	3.1	20
409	Flexible Energy Storage Device Based on Poly( <i>N</i> -phenylglycine), an Incentive-Energy Pseudocapacitive Conducting Polymer, and Electrochemically Exfoliated Graphite Sheets. ACS Sustainable Chemistry and Engineering, 2020, 8, 6433-6441.	6.7	20
410	Cobalt sulfide-reduced graphene oxide: An efficient catalyst for the degradation of rhodamine B and pentachlorophenol using peroxymonosulfate. Journal of Environmental Chemical Engineering, 2021, 9, 106018.	6.7	20
411	Nanopatterning of Si(111) surfaces by atomic force microscope scratching of an organic monolayer. Electrochemistry Communications, 2003, 5, 337-340.	4.7	19
412	Investigation of the electrocatalytic activity of boron-doped diamond electrodes modified with palladium or gold nanoparticles for oxygen reduction reaction in basic medium. Comptes Rendus Chimie, 2008, 11, 1004-1009.	0.5	19
413	Application of Thin Titanium/Titanium Oxide Layers Deposited on Gold for Infrared Reflection Absorption Spectroscopy: Structural Studies of Lipid Bilayers. Langmuir, 2008, 24, 7378-7387.	3.5	19
414	Optical and electrochemical properties of tunable host–guest complexes linked to plasmonic interfaces. Journal of Materials Chemistry, 2011, 21, 3006.	6.7	19

#	Article	IF	CITATIONS
415	An impedimetric immunosensor based on diamond nanowires decorated with nickel nanoparticles. Analyst, The, 2014, 139, 1726.	3.5	19
416	Production Rate and Reactivity of Singlet Oxygen1O2(1Δg) Directly Photoactivated at 1270 nm in Lipid Nanocapsules Dispersed in Water. Journal of Physical Chemistry C, 2014, 118, 2885-2893.	3.1	19
417	Controllable fabrication of stable superhydrophobic surfaces on iron substrates. RSC Advances, 2015, 5, 40657-40667.	3.6	19
418	Excellent photocatalytic reduction of nitroarenes to aminoarenes by BiVO <sub>4</sub> nanoparticles grafted on reduced graphene oxide (rGO/BiVO <sub>4</sub> ). Applied Organometallic Chemistry, 2019, 33, e5059.	3.5	19
419	Palladium oxide nanoparticles supported on graphene oxide: A convenient heterogeneous catalyst for reduction of various carbonyl compounds using triethylsilane. Applied Organometallic Chemistry, 2019, 33, e4837.	3.5	19
420	Cu <sub>2</sub> O/reduced graphene oxide/TiO <sub>2</sub> nanomaterial: An effective photocatalyst for azideâ€alkyne cycloaddition with benzyl halides or epoxide derivatives under visible light irradiation. Applied Organometallic Chemistry, 2020, 34, e5928.	3.5	19
421	High-performance flexible hybrid supercapacitor based on NiAl layered double hydroxide as a positive electrode and nitrogen-doped reduced graphene oxide as a negative electrode. Electrochimica Acta, 2020, 354, 136664.	5.2	19
422	Localized Surface Plasmon Resonance of Gold Nanoparticle-Modified Chitosan Films for Heavy-Metal Ions Sensing. Journal of Nanoscience and Nanotechnology, 2009, 9, 350-357.	0.9	18
423	Development of New Localized Surface Plasmon Resonance Interfaces Based on Gold Nanostructures Sandwiched between Tin-Doped Indium Oxide Films. Langmuir, 2010, 26, 4266-4273.	3.5	18
424	Cell Adhesion Properties on Chemically Micropatterned Boron-Doped Diamond Surfaces. Langmuir, 2010, 26, 15065-15069.	3.5	18
425	Silica Cross-linked Micelles Loading with Silicon Nanoparticles: Preparation and Characterization. ACS Applied Materials & Interfaces, 2013, 5, 7042-7049.	8.0	18
426	Split and flow: reconfigurable capillary connection for digital microfluidic devices. Lab on A Chip, 2014, 14, 3589-3593.	6.0	18
427	Formation of a Highly Stable and Nontoxic Protein Corona upon Interaction of Human α-1-Acid Glycoprotein (AGP) with Citrate-Stabilized Silver Nanoparticles. Langmuir, 2020, 36, 10321-10330.	3.5	18
428	SERS characterization of aggregated and isolated bacteria deposited on silver-based substrates. Analytical and Bioanalytical Chemistry, 2021, 413, 1417-1428.	3.7	18
429	Far-UV laser flash photolysis in solution. A study of the chemistry of 1,1-dimethylsilene in hydrocarbon solvents. Journal of Photochemistry and Photobiology A: Chemistry, 1997, 110, 243-246.	3.9	17
430	Preparation and Characterization of Decyl-Terminated Silicon Nanoparticles Encapsulated in Lipid Nanocapsules. Langmuir, 2013, 29, 12688-12696.	3.5	17
431	Electroless chemical etching of silicon in aqueous NH4F/AgNO3/HNO3 solution. Applied Surface Science, 2013, 284, 894-899.	6.1	17
432	Particle-based photodynamic therapy based on indocyanine green modified plasmonic nanostructures for inactivation of a Crohn's disease-associated Escherichia coli strain. Journal of Materials Chemistry B, 2016, 4, 2598-2605.	5.8	17

#	Article	IF	CITATIONS
433	Plasmon-Induced Electrocatalysis with Multi-Component Nanostructures. Materials, 2019, 12, 43.	2.9	17
434	The Influence of Microstructure on the Passive Layer Chemistry and Corrosion Resistance for Some Titanium-Based Alloys. Materials, 2019, 12, 1233.	2.9	17
435	Surface Functionalization with Polyethylene Glycol and Polyethyleneimine Improves the Performance of Graphene-Based Materials for Safe and Efficient Intracellular Delivery by Laser-Induced Photoporation. International Journal of Molecular Sciences, 2020, 21, 1540.	4.1	17
436	The holy grail of pyrene-based surface ligands on the sensitivity of graphene-based field effect transistors. Sensors & Diagnostics, 2022, 1, 235-244.	3.8	17
437	Effects of natural and electrochemical oxidation processes on acoustic waves in porous silicon films. Journal of Applied Physics, 2003, 94, 1243-1247.	2.5	16
438	Chemical and electrochemical grafting of polyaniline on anilineâ€ŧerminated porous silicon. Surface and Interface Analysis, 2010, 42, 1342-1346.	1.8	16
439	Characterization of the state of a droplet on a micro-textured silicon wafer using ultrasound. Journal of Applied Physics, 2012, 112, .	2.5	16
440	Direct oxidative synthesis of nitrones from aldehydes and primary anilines using graphite oxide and Oxone. Tetrahedron Letters, 2014, 55, 5471-5474.	1.4	16
441	Green Synthesis of Reduced Graphene Oxide-Silver Nanoparticles Using Environmentally Friendly L-arginine for H <sub>2</sub> O <sub>2</sub> Detection. ECS Journal of Solid State Science and Technology, 2016, 5, M3060-M3066.	1.8	16
442	Affinity of Glycanâ€Modified Nanodiamonds towards Lectins and Uropathogenic <i>Escherichia Coli</i> . ChemNanoMat, 2016, 2, 307-314.	2.8	16
443	Vertically Aligned Nitrogen-Doped Carbon Nanotube Carpet Electrodes: Highly Sensitive Interfaces for the Analysis of Serum from Patients with Inflammatory Bowel Disease. ACS Applied Materials & Interfaces, 2016, 8, 9600-9609.	8.0	16
444	Catalytic activity of silicon nanowires decorated with silver and copper nanoparticles. Semiconductor Science and Technology, 2016, 31, 014011.	2.0	16
445	Evaporation of nanofluid sessile drops: Infrared and acoustic methods to track the dynamic deposition of copper oxide nanoparticles. International Journal of Heat and Mass Transfer, 2018, 127, 1168-1177.	4.8	16
446	Rapid and sensitive identification of uropathogenic Escherichia coli using a surface-enhanced-Raman-scattering-based biochip. Talanta, 2020, 219, 121174.	5.5	16
447	Graphene Oxide Nanosheets for Localized Hyperthermia—Physicochemical Characterization, Biocompatibility, and Induction of Tumor Cell Death. Cells, 2020, 9, 776.	4.1	16
448	Modification of MnFe2O4 surface by Mo (VI) pyridylimine complex as an efficient nanocatalyst for (ep)oxidation of alkenes and sulfides. Journal of Molecular Liquids, 2021, 330, 115690.	4.9	16
449	Self-combustion synthesis of dilithium cobalt bis(tungstate) decorated with silver nanoparticles for high performance hybrid supercapacitors. Chemical Engineering Journal, 2021, 426, 131252.	12.7	16
450	Surface Plasmon Resonance (SPR) for the Evaluation of Shear-Force-Dependent Bacterial Adhesion. Biosensors, 2015, 5, 276-287.	4.7	15

#	Article	IF	CITATIONS
451	Plasmon waveguide resonance for sensing glycan–lectin interactions. Analytica Chimica Acta, 2015, 873, 71-79.	5.4	15
452	Infrared Photothermal Therapy with Water Soluble Reduced Graphene Oxide: Shape, Size and Reduction Degree Effects. Nano LIFE, 2015, 05, 1540002.	0.9	15
453	Visible light assisted hydrogen generation from complete decomposition of hydrous hydrazine using rhodium modified TiO2 photocatalysts. Photochemical and Photobiological Sciences, 2017, 16, 1036-1042.	2.9	15
454	Porous reduced graphene oxide modified electrodes for the analysis of protein aggregation. Part 1: Lysozyme aggregation at pH 2 and 7.4. Electrochimica Acta, 2017, 254, 375-383.	5.2	15
455	Visible light assisted oxidative coupling of benzylamines using heterostructured nanocomposite photocatalyst. Journal of Photochemistry and Photobiology A: Chemistry, 2018, 356, 457-463.	3.9	15
456	Magnetically Reusable MnFe <sub>2</sub> O <sub>4</sub> Nanoparticles Modified with Oxoâ€Peroxo Mo (VI) Schiffâ€Base Complexes: A High Efficiency Catalyst for Olefin Epoxidation under Solventâ€Free Conditions. ChemistrySelect, 2018, 3, 2877-2881.	1.5	15
457	Improved photodynamic effect through encapsulation of two photosensitizers in lipid nanocapsules. Journal of Materials Chemistry B, 2018, 6, 5949-5963.	5.8	15
458	"Click―Chemistry on Gold Electrodes Modified with Reduced Graphene Oxide by Electrophoretic Deposition. Surfaces, 2019, 2, 193-204.	2.3	15
459	Enhanced visible light-triggered antibacterial activity of carbon quantum dots/polyurethane nanocomposites by gamma rays induced pre-treatment. Radiation Physics and Chemistry, 2021, 185, 109499.	2.8	15
460	SILA- AND GERMACYCLOPENTENES IN FUNDAMENTAL AND APPLIED ORGANOMETALLIC CHEMISTRY. Main Group Metal Chemistry, 1996, 19, .	1.6	14
461	Pickled luminescent silicon nanostructures. Solid State Communications, 2001, 118, 319-323.	1.9	14
462	Stable electroluminescence from passivated nano-crystalline porous silicon using undecylenic acid. Physica Status Solidi C: Current Topics in Solid State Physics, 2005, 2, 3273-3277.	0.8	14
463	In situmonitoring of protein adsorption on functionalized porous Si surfaces. Journal of Vacuum Science and Technology A: Vacuum, Surfaces and Films, 2006, 24, 747-751.	2.1	14
464	The collagen assisted self-assembly of silicon nanowires. Nanotechnology, 2009, 20, 235601.	2.6	14
465	Electrowetting on functional fibers. Soft Matter, 2013, 9, 492-497.	2.7	14
466	Graphite oxide-promoted one-pot synthesis and oxidative aromatization of Hantzsch 1,4-dihydropyridines. Monatshefte Für Chemie, 2014, 145, 1919-1924.	1.8	14
467	Formation of nanostructured silicon surfaces by stain etching. Nanoscale Research Letters, 2014, 9, 482.	5.7	14
468	One-pot green synthesis of reduced graphene oxide decorated with β-Ni(OH)2-nanoflakes as an efficient electrochemical platform for the determination of antipsychotic drug sulpiride. Microchemical Journal, 2019, 147, 555-563.	4.5	14

#	Article	IF	CITATIONS
469	Preparation of boron-doped diamond nanospikes on porous Ti substrate for high-performance supercapacitors. Electrochimica Acta, 2020, 354, 136649.	5.2	14
470	Long-term live-cell microscopy with labeled nanobodies delivered by laser-induced photoporation. Nano Research, 2020, 13, 485-495.	10.4	14
471	Interaction of cellulose and nitrodopamine coated superparamagnetic iron oxide nanoparticles with alpha-lactalbumin. RSC Advances, 2020, 10, 9704-9716.	3.6	14
472	Carbon quantum dots as a dual platform for the inhibition and light-based destruction of collagen fibers: implications for the treatment of eye floaters. Nanoscale Horizons, 2021, 6, 449-461.	8.0	14
473	Synthesis and characterization of palladium nanoparticles immobilized on graphene oxide functionalized with triethylenetetramine or 2,6-diaminopyridine and application for the Suzuki cross-coupling reaction. Journal of Organometallic Chemistry, 2022, 957, 122160.	1.8	14
474	Photothermal Activatable Mucoadhesive Fiber Mats for On-Demand Delivery of Insulin via Buccal and Corneal Mucosa. ACS Applied Bio Materials, 2022, 5, 771-778.	4.6	14
475	Synthesis and characterization of a novel multi-functionalized reduced graphene oxide as a pH-sensitive drug delivery material and a photothermal candidate. Applied Surface Science, 2022, 583, 152568.	6.1	14
476	Adsorption-reduction of Cr(VI) onto unmodified and phytic acid-modified carob waste: Kinetic and isotherm modeling. Chemosphere, 2022, 297, 134188.	8.2	14
477	Regioselectivity in the trichlorosilylation of allylic halides. Synthesis of 1,1-dichloro-3-(methyldichlorosilyl)-1-silacyclopent-3-ene. Journal of Organometallic Chemistry, 1993, 444, 37-40.	1.8	13
478	Alkyl passivation and SiO2 encapsulation of silicon nanoparticles: preparation, surface modification and luminescence properties. Journal of Materials Chemistry C, 2013, 1, 5261.	5.5	13
479	Droplet transport by electrowetting: lets get rough!. Microfluidics and Nanofluidics, 2013, 15, 327-336.	2.2	13
480	Fabrication of stable homogeneous superhydrophobic HDPE/graphene oxide surfaces on zinc substrates. RSC Advances, 2016, 6, 29823-29829.	3.6	13
481	Atomic Force Microscopic and Raman Investigation of Boron-Doped Diamond Nanowire Electrodes and Their Activity toward Oxygen Reduction. Journal of Physical Chemistry C, 2017, 121, 3397-3403.	3.1	13
482	On demand electrochemical release of drugs from porous reduced graphene oxide modified flexible electrodes. Journal of Materials Chemistry B, 2017, 5, 6557-6565.	5.8	13
483	Magneto-Optical Nanostructures for Viral Sensing. Nanomaterials, 2020, 10, 1271.	4.1	13
484	Enhanced electrocatalytic activity of PtRu/nitrogen and sulphur co-doped crumbled graphene in acid and alkaline media. Journal of Colloid and Interface Science, 2021, 590, 154-163.	9.4	13
485	Graphene-Induced Hyperthermia (GIHT) Combined With Radiotherapy Fosters Immunogenic Cell Death. Frontiers in Oncology, 2021, 11, 664615.	2.8	13
486	Emerging advances and current applications of nanoMOF-based membranes for water treatment. Chemosphere, 2022, 292, 133369.	8.2	13

#	Article	IF	CITATIONS
487	3,4-Functionalized silacyclopentanes. Synthesis of trans-4-amino-, azido- and alkyloxy-1-silacyclopentan-3-ols from 6-oxa-3-silabicyclo[3.1.0]hexanes. Journal of Organometallic Chemistry, 1994, 484, 119-127.	1.8	12
488	Stereoselective synthesis of new hetero(P, Si, Ge, Sn)cyclic derivatives from zirconium diyne and diene complexes. Journal of Organometallic Chemistry, 1998, 564, 61-70.	1.8	12
489	Plasmonic properties of silver nanostructures coated with an amorphous silicon–carbon alloy and their applications for sensitive sensing of DNA hybridization. Analyst, The, 2011, 136, 1859.	3.5	12
490	Amino-Functionalized MCM-41 base-Catalyzed one-Pot synthesis of 2-Amino-5,6-dihydropyrimidin-4(3H)-ones. Journal of the Iranian Chemical Society, 2011, 8, 280-286.	2.2	12
491	Simple and low-cost fabrication of PDMS microfluidic round channels by surface-wetting parameters optimization. Microfluidics and Nanofluidics, 2012, 12, 953-961.	2.2	12
492	Investigation of morphology, reflectance and photocatalytic activity of nanostructured silicon surfaces. Microelectronic Engineering, 2016, 159, 94-101.	2.4	12
493	Short-term exposure to gold nanoparticle suspension impairs swimming behavior in a widespread calanoid copepod. Environmental Pollution, 2017, 228, 102-110.	7.5	12
494	Graphite/Nanocrystalline Zeolite Platform for Selective Electrochemical Determination of Hepatitis C Inhibitor Ledipasvir. Electroanalysis, 2019, 31, 1215-1223.	2.9	12
495	Plasmon-enhanced electrocatalytic oxygen reduction in alkaline media on gold nanohole electrodes. Journal of Materials Chemistry A, 2020, 8, 10395-10401.	10.3	12
496	Morphological influence of BiVO4 nanostructures on peroxymonosulfate activation for highly efficient catalytic degradation of rhodamine B. Environmental Science and Pollution Research, 2021, 28, 52236-52246.	5.3	12
497	Flowerâ€like Nitrogenâ€coâ€doped MoS <sub>2</sub> @RGO Composites with Excellent Stability for Supercapacitors. ChemElectroChem, 2021, 8, 2903-2911.	3.4	12
498	Covalent functionalization of silicon nitride surfaces by semicarbazide group. Surface Science, 2007, 601, 5492-5498.	1.9	11
499	Me <sub>3</sub> SiCl and Et <sub>3</sub> Silâ€promoted oneâ€pot synthesis of 1,4â€dihydropyridine derivatives. Applied Organometallic Chemistry, 2009, 23, 267-271.	3.5	11
500	Cheap and Efficient Protocol for the Synthesis of Tetrahydroquinazolinone, Dihydropyrimidinone, and Pyrimidinone Derivatives. Synthetic Communications, 2009, 40, 8-20.	2.1	11
501	A convenient and efficient one-pot method for the synthesis of novel acridine-calix[4]arene derivatives as new DNA binding agents via multicomponent reaction. Supramolecular Chemistry, 2014, 26, 442-449.	1.2	11
502	Lipid nanocapsules containing the non-ionic surfactant Solutol HS15 inhibit the transport of calcium through hyperforin-activated channels in neuronal cells. Neuropharmacology, 2015, 99, 726-734.	4.1	11
503	Differentiation of Crohn's Disease-Associated Isolates from Other Pathogenic Escherichia coli by Fimbrial Adhesion under Shear Force. Biology, 2016, 5, 14.	2.8	11
504	High photocatalytic activity of plasmonic Ag@AgCl/Zn <sub>2</sub> SnO <sub>4</sub> nanocomposites synthesized using hydrothermal method. RSC Advances, 2016, 6, 80310-80319.	3.6	11

#	Article	IF	CITATIONS
505	Lipid nanocapsules for behavioural testing in aquatic toxicology: Time–response of Eurytemora affinis to environmental concentrations of PAHs and PCB. Aquatic Toxicology, 2016, 170, 310-322.	4.0	11
506	Wilkinsonâ€Type Immobilized Catalyst on Diamond Nanoparticles for Alkene Reduction. ChemCatChem, 2017, 9, 432-439.	3.7	11
507	Chitosan/hydroxyapatite modified carbon/carbon composites: synthesis, characterization and <i>in vitro</i> biocompatibility evaluation. RSC Advances, 2019, 9, 23362-23372.	3.6	11
508	New Bacteriocins from Lacticaseibacillus paracasei CNCM I-5369 Adsorbed on Alginate Nanoparticles Are Very Active against Escherichia coli. International Journal of Molecular Sciences, 2020, 21, 8654.	4.1	11
509	Copperâ€based metal–organic framework decorated by CuO hairâ€like nanostructures: Electrocatalyst for oxygen evolution reaction. Applied Organometallic Chemistry, 2020, 34, e5871.	3.5	11
510	Crystalline <scp>ZnO</scp> and <scp>ZnO</scp>   <scp> TiO <sub>2</sub> </scp> nanoparticles derived from <i>tert</i> â€butyl Nâ€(2 mercaptoethyl)carbamatozinc( <scp>II</scp> ) chelate: Electrocatalytic studies for <scp> H <sub>2</sub> </scp> generation in alkaline electrolytes. International Journal of Energy Research, 2020, 44, 6725-6744.	4.5	11
511	Enhanced Antibacterial Activity of CuS-BSA/Lysozyme under Near Infrared Light Irradiation. Nanomaterials, 2021, 11, 2156.	4.1	11
512	The importance of the shape of Cu2O nanocrystals on plasmon-enhanced oxygen evolution reaction in alkaline media. Electrochimica Acta, 2021, 390, 138810.	5.2	11
513	Porous silica-laser dye composite: physical and optical properties. Physica Status Solidi (A) Applications and Materials Science, 2007, 204, 1518-1522.	1.8	10
514	Preparation and characterization of thin organosilicon films deposited on SPR chip. Electrochimica Acta, 2008, 53, 3910-3915.	5.2	10
515	Electrochemical investigation of the influence of thin SiOx films deposited on gold on charge transfer characteristics. Electrochimica Acta, 2008, 53, 7908-7914.	5.2	10
516	Solvent-free chemical functionalization of hydrogen-terminated boron-doped diamond electrodes with diazonium salts in ionic liquids. Diamond and Related Materials, 2008, 17, 1394-1398.	3.9	10
517	Wet-chemical approach for the halogenation of hydrogenated boron-doped diamond electrodes. Chemical Communications, 2008, , 6294.	4.1	10
518	Palladium atalyzed reduction of nitroaromatic compounds to the corresponding anilines. Applied Organometallic Chemistry, 2010, 24, 477-480.	3.5	10
519	Direct Characterization of Native Chemical Ligation of Peptides on Silicon Nanowires. Langmuir, 2012, 28, 13336-13344.	3.5	10
520	Lithographically patterned silicon nanostructures on silicon substrates. Applied Surface Science, 2012, 258, 6007-6012.	6.1	10
521	Characterization of peptide attachment on silicon nanowires by X-ray photoelectron spectroscopy and mass spectrometry. Analyst, The, 2017, 142, 969-978.	3.5	10
522	Substance P enhances lactic acid and tyramine production in Enterococcus faecalis V583 and promotes its cytotoxic effect on intestinal Caco-2/TC7 cells. Gut Pathogens, 2017, 9, 20.	3.4	10

#	Article	IF	CITATIONS
523	Dopamine-functionalized cyclodextrins: modification of reduced graphene oxide based electrodes and sensing of folic acid in human serum. Analytical and Bioanalytical Chemistry, 2019, 411, 5149-5157.	3.7	10
524	High spatial resolution electrochemical biosensing using reflected light microscopy. Scientific Reports, 2019, 9, 15196.	3.3	10
525	Mucin modified SPR interfaces for studying the effect of flow on pathogen binding to Atlantic salmon mucins. Biosensors and Bioelectronics, 2019, 146, 111736.	10.1	10
526	Interaction of Human α-1-Acid Glycoprotein (AGP) with Citrate-Stabilized Gold Nanoparticles: Formation of Unexpectedly Strong Binding Events. Journal of Physical Chemistry C, 2019, 123, 5073-5083.	3.1	10
527	MnOx thin film based electrodes: Role of surface point defects and structure towards extreme enhancement in specific capacitance. Materials Chemistry and Physics, 2020, 242, 122487.	4.0	10
528	Enhanced electrocatalytic hydrogen evolution on a plasmonic electrode: the importance of the Ti/TiO2 adhesion layer. Journal of Materials Chemistry A, 2020, 8, 13980-13986.	10.3	10
529	Magnetic MnFe2O4 Core–shell nanoparticles coated with antibiotics for the ablation of pathogens. Chemical Papers, 2021, 75, 377-387.	2.2	10
530	Rapid Generation of Coronaviral Immunity Using Recombinant Peptide Modified Nanodiamonds. Pathogens, 2021, 10, 861.	2.8	10
531	Alginate Nanoparticles Enhance Anti-Clostridium perfringens Activity of the Leaderless Two-Peptide Enterocin DD14 and Affect Expression of Some Virulence Factors. Probiotics and Antimicrobial Proteins, 2021, 13, 1213-1227.	3.9	10
532	Surface modification of carbon dots with tetraalkylammonium moieties for fine tuning their antibacterial activity. Materials Science and Engineering C, 2022, 134, 112697.	7.3	10
533	Synthèses de 3-silyl et de 3-germyl 1-sila et 1-germacyclopent-3-ènes. Journal of Organometallic Chemistry, 1993, 460, 155-161.	1.8	9
534	Steady state and time-resolved spectroscopic studies of the photochemistry of 1-arylsilacyclobutanes and the chemistry of 1-arylsilenes. Canadian Journal of Chemistry, 1999, 77, 1136-1147.	1.1	9
535	A Brillouin scattering study of the effect of chemical passivation on the elastic properties of porous silicon. Semiconductor Science and Technology, 2002, 17, 692-695.	2.0	9
536	Bulk micromachining of silicon using electron-beam-induced carbonaceous nanomasking. Nanotechnology, 2006, 17, 5363-5366.	2.6	9
537	Electro-oxidative nanopatterning of silane monolayers on boron-doped diamond electrodes. Nanotechnology, 2009, 20, 075302.	2.6	9
538	Wet Chemical Approaches for Chemical Functionalization of Semiconductor Nanostructures. Nanostructure Science and Technology, 2009, , 183-248.	0.1	9
539	Characterization of single transition metal oxide nanorods by combining atomic force microscopy and polarized micro-Raman spectroscopy. Chemical Physics Letters, 2011, 514, 128-133.	2.6	9
540	Ferromagnetism induced in ZnO nanorods by morphology changes under a nitrogen–carbon atmosphere. RSC Advances, 2013, 3, 12945.	3.6	9

#	Article	IF	CITATIONS
541	Decoration of silicon nanostructures with copper particles for simultaneous selective capture and mass spectrometry detection of His-tagged model peptide. Analyst, The, 2014, 139, 5155-5163.	3.5	9
542	Light-Triggered Release of Biomolecules from Diamond Nanowire Electrodes. Langmuir, 2016, 32, 6515-6523.	3.5	9
543	Preparation of Low-Resistance and Residue-free ITO Films for Large-scale 3D Displays. ACS Applied Materials & Interfaces, 2019, 11, 45903-45913.	8.0	9
544	Mussel-Inspired Superhydrophobic Surfaces on 316L Stainless Steel with Enhanced Corrosion Resistance. Metallurgical and Materials Transactions A: Physical Metallurgy and Materials Science, 2020, 51, 909-919.	2.2	9
545	Cathodic activation of synthesized highly defective monoclinic hydroxylâ€functionalized <scp> ZrO <sub>2</sub> </scp> nanoparticles for efficient electrochemical production of hydrogen in alkaline media. International Journal of Energy Research, 2020, 44, 10695-10709.	4.5	9
546	Ultrasound Assisted the Synthesis of 1,3-Dioxolane Derivatives from the Reaction of Epoxides or 1,2-Diols with Various Ketones Using Graphene Oxide Catalyst. Catalysis Letters, 2020, 150, 2959-2969.	2.6	9
547	Electrochemical and electronic detection of biomarkers in serum: a systematic comparison using aptamer-functionalized surfaces. Analytical and Bioanalytical Chemistry, 2022, 414, 5319-5327.	3.7	9
548	TRPM8 as an Anti–Tumoral Target in Prostate Cancer Growth and Metastasis Dissemination. International Journal of Molecular Sciences, 2022, 23, 6672.	4.1	9
549	Determination of coverage in passivated porous silicon by Brillouin spectroscopy. Applied Physics Letters, 2001, 79, 4521-4523.	3.3	8
550	Graphene-based high-performance surface plasmon resonance biosensors. Proceedings of SPIE, 2012, , .	0.8	8
551	Investigation of the anti-biofouling properties of graphene oxide aqueous solutions by electrowetting characterization. Journal of Materials Chemistry A, 2013, 1, 12355.	10.3	8
552	Diamond nanowires modified with poly[3-(pyrrolyl)carboxylic acid] for the immobilization of histidine-tagged peptides. Analyst, The, 2014, 139, 4343.	3.5	8
553	Surface modification of semiconducting silicon nanowires for biosensing applications. , 2014, , 26-61.		8
554	Fast and facile preparation of nanostructured silicon surfaces for laser desorption/ionization mass spectrometry of small compounds. Rapid Communications in Mass Spectrometry, 2019, 33, 66-74.	1.5	8
555	High performance of 3D silicon nanowires array@CrN for electrochemical capacitors. Nanotechnology, 2020, 31, 035407.	2.6	8
556	Electrochemical, theoretical and surface physicochemical studies of the alkaline copper corrosion inhibition by newly synthesized molecular complexes of benzenediamine and tetraamine with π acceptor. Journal of Molecular Liquids, 2020, 320, 114386.	4.9	8
557	Aryne cycloaddition reaction as a facile and mild modification method for design of electrode materials for high-performance symmetric supercapacitor. Electrochimica Acta, 2021, 369, 137667.	5.2	8
558	The Potential of Developing Pan-Coronaviral Antibodies to Spike Peptides in Convalescent COVID-19 Patients. Archivum Immunologiae Et Therapiae Experimentalis, 2021, 69, 5.	2.3	8

#	Article	IF	CITATIONS
559	Cathodic pre-polarization studies on the carbon felt/KOH interface: An efficient metal-free electrocatalyst for hydrogen generation. Electrochimica Acta, 2021, 375, 137981.	5.2	8
560	Facile and secure synthesis of porous partially fluorinated graphene employing weakly coordinating anion for enhanced high-performance symmetric supercapacitor. Journal of Materiomics, 2022, 8, 113-122.	5.7	8
561	An efficient CuO/rGO/TiO <sub>2</sub> photocatalyst for the synthesis of benzopyranopyrimidine compounds under visible light irradiation. New Journal of Chemistry, 2022, 46, 3817-3830.	2.8	8
562	Les Sels de Bismuth (III) Comme Catalyseurs Dans la Reaction D'ouverture Des Epoxydes en Sere Siliciee. Phosphorus, Sulfur and Silicon and the Related Elements, 2000, 167, 81-92.	1.6	7
563	Organic monolayers detected by single reflection attenuated total reflection infrared spectroscopy. Journal of Vacuum Science and Technology A: Vacuum, Surfaces and Films, 2006, 24, 668-672.	2.1	7
564	Fabrication of silicon nanostructures using metalâ€assisted etching in NaBF <sub>4</sub> . Physica Status Solidi (A) Applications and Materials Science, 2013, 210, 2178-2182.	1.8	7
565	3D silicon shapes through bulk nano structuration by focused ion beam implantation and wet etching. Nanotechnology, 2017, 28, 205301.	2.6	7
566	Room-Temperature Wet Chemical Synthesis of Au NPs/TiH2/Nanocarved Ti Self-Supported Electrocatalysts for Highly Efficient H2 Generation. ACS Applied Materials & Interfaces, 2017, 9, 30115-30126.	8.0	7
567	Graphene-based bioelectrochemistry and bioelectronics: A concept for the future?. Current Opinion in Electrochemistry, 2018, 12, 141-147.	4.8	7
568	Pt–ZnO/M (M = Fe, Co, Ni or Cu): A New Promising Hybrid-Doped Noble Metal/Semiconductor Photocatalysts. Journal of Inorganic and Organometallic Polymers and Materials, 2020, 30, 4627-4636.	3.7	7
569	Efficacious Alkaline Copper Corrosion Inhibition by a Mixed Ligand Copper(II) Complex of 2,2′â€Bipyridine and Glycine: Electrochemical and Theoretical Studies. ChemElectroChem, 2021, 8, 2052-2064.	3.4	7
570	Construction of a bone-like surface layer on hydroxyl-modified carbon/carbon composite implants via biomimetic mineralization and in vivo tests. RSC Advances, 2016, 6, 9370-9378.	3.6	7
571	Chemical and thermal stability of titanium disilicide contacts on silicon. Journal of Applied Physics, 2001, 90, 1655-1659.	2.5	6
572	One-pot synthesis of 2-aminotetrahydrothiopyrano[4,3-b]pyran-3-carbonitrile derivatives using mesoporous NH2-MCM-41. Monatshefte Für Chemie, 2013, 144, 1699-1704.	1.8	6
573	Search of Extremely Sensitive Near-Infrared Plasmonic Interfaces: A Theoretical Study. Plasmonics, 2013, 8, 1691-1698.	3.4	6
574	Photochemical reaction of vitamin C with silicon nanocrystals: polymerization, hydrolysis and photoluminescence. Journal of Materials Chemistry C, 2013, 1, 5856.	5.5	6
575	Palladium(II) acetateâ€catalyzed reduction of imines to the corresponding amines by triethylsilane. Applied Organometallic Chemistry, 2013, 27, 174-176.	3.5	6
576	Enhanced Photoluminescence in Acetylene-Treated ZnO Nanorods. Nanoscale Research Letters, 2016, 11, 413.	5.7	6

#	Article	IF	CITATIONS
577	Manganese Ferrite Nanoparticles Modified by Mo(VI) Complex: Highly Efficient Catalyst for Sulfides and Olefins Oxidation Under Solventâ€less Condition. ChemistrySelect, 2019, 4, 7116-7122.	1.5	6
578	The antimicrobial peptide oranicin P16 isolated from Trichosporon asahii ICVY021, found in camel milk's, inhibits Kocuria rhizophila. Food Bioscience, 2020, 36, 100670.	4.4	6
579	Silicon nanowire-hydrogenated TiO2 core-shell arrays for stable electrochemical micro-capacitors. Electrochimica Acta, 2021, 396, 139198.	5.2	6
580	Single‣tep Synthesis of Exfoliated Ti <sub>3</sub> C <sub>2</sub> T <sub>x</sub> MXene through NaBF <sub>4</sub> /HCl Etching as Electrode Material for Asymmetric Supercapacitor. ChemistrySelect, 2022, 7, .	1.5	6
581	NMR Spectra of Organogermanium Compounds. Part XII.73Ge and13C NMR Spectra and Molecular Mechanics Calculations of 3-Germabicyclo[3.1.0]hexanes and Related Compounds. Bulletin of the Chemical Society of Japan, 1993, 66, 1732-1737.	3.2	5
582	Structure Characterization of Porous Silicon Layers Based on a Theoretical Analysis. Langmuir, 2002, 18, 4165-4170.	3.5	5
583	Effect of ruthenium cluster on the photoluminescence of chemically derivatized porous silicon. Applied Surface Science, 2003, 217, 125-133.	6.1	5
584	Preparation and reactivity of carboxylic acid-terminated boron-doped diamond electrodes. Electrochimica Acta, 2010, 55, 959-964.	5.2	5
585	Localized surface plasmon resonance interfaces coated with poly[3-(pyrrolyl)carboxylic acid] for histidine-tagged peptide sensing. Analyst, The, 2011, 136, 4211.	3.5	5
586	A graphene/hemin hybrid material as an efficient green catalyst for stereoselective olefination of aldehydes. RSC Advances, 2015, 5, 100011-100017.	3.6	5
587	Comparison of Ti-Based Coatings on Silicon Nanowires for Phosphopeptide Enrichment and Their Laser Assisted Desorption/Ionization Mass Spectrometry Detection. Nanomaterials, 2017, 7, 272.	4.1	5
588	Porous reduced graphene oxide modified electrodes for the analysis of protein aggregation. Part 2: Application to the analysis of calcitonin containing pharmaceutical formulation. Electrochimica Acta, 2018, 266, 364-372.	5.2	5
589	Carbon–nitrogen bond formation using modified graphene oxide derivatives decorated with copper complexes and nanoparticles. Applied Organometallic Chemistry, 2021, 35, e6327.	3.5	5
590	STUDY OF THE REGIOSELECTIVITY OF THE TRICHLOROSILYLATION OF ALLYLIC HALIDES. NOVEL 3-SILYL AND 3-GERMYL-1-SILA-3-CYCLOPENTENES. Main Group Metal Chemistry, 1994, 17, .	1.6	4
591	Synthesis and characterization of poly(1-sila-cis-pent-3-enes) substituted with pendant pyridinyl groups. Journal of Inorganic and Organometallic Polymers, 1995, 5, 61-74.	1.5	4
592	A MODIFIED McCORMACK SYNTHESIS OF 3-SILYLATED PHOSPHOL-3-ENES. Phosphorus, Sulfur and Silicon and the Related Elements, 1995, 105, 101-108.	1.6	4
593	1Η NMR SPECTRA OF 3-GERMABICYCLO[3.1.0]HEXANES AND 6-OXA-3-GERMABICYCLO[3.1.0]HEXANES. Main Group Metal Chemistry, 1995, 18, .	1.6	4
594	Unprecedented effects of the trimethylsilyl group on the reactivity of 3C-silylated silacyclopentenes and their derivatives. Journal of Organometallic Chemistry, 2000, 604, 141-149.	1.8	4

#	Article	IF	CITATIONS
595	Infrared spectroscopy of self-assembled monolayer films on silicon. Surface Science, 2007, 601, 2566-2570.	1.9	4
596	Palladium chloride-catalyzed reductive cleavage of benzylic acetal, ketal and ether compounds with triethylsilane. Journal of the Iranian Chemical Society, 2011, 8, 570-573.	2.2	4
597	Preparation and photocatalytic properties of quartz/gold nanostructures/TiO2 lamellar structures. RSC Advances, 2012, 2, 12482.	3.6	4
598	Investigation of the corrosion behaviour of steel coated with amorphous silicon carbon alloys. Surface and Coatings Technology, 2012, 206, 3626-3631.	4.8	4
599	Amino-functionalized SBA-15 catalyzed one-step synthesis of 2-amino-5-cyano-4-hydroxy-6-aryl pyrimidines. Journal of the Iranian Chemical Society, 2013, 10, 559-563.	2.2	4
600	Chapter 7. Electrochemistry of graphene: The current state of the art. SPR Electrochemistry, 0, , 211-242.	0.7	4
601	Functionalization of diamond surfaces for medical applications. , 2013, , 25-47.		4
602	Biocompatibility of semiconducting silicon nanowires. , 2014, , 62-85.		4
603	Lipid nanocapsules as a new delivery system in copepods: Toxicity studies and optical imaging. Colloids and Surfaces B: Biointerfaces, 2015, 135, 441-447.	5.0	4
604	Interaction of 4 allotropic modifications of carbon nanoparticles with living tissues. Ukrainian Biochemical Journal, 2019, 91, 41-50.	0.5	4
605	Combining combing and secondary ion mass spectrometry to study DNA on chips using 13C and 15N labeling. F1000Research, 2016, 5, 1437.	1.6	4
606	Catch and release strategy of matrix metalloprotease aptamers <i>via</i> thiol–disulfide exchange reaction on a graphene based electrochemical sensor. Sensors & Diagnostics, 2022, 1, 739-749.	3.8	4
607	Spiro[3-germabicyclo[3.1.0]hexane-3,9'-[9]germafluorene]. Acta Crystallographica Section C: Crystal Structure Communications, 1994, 50, 1337-1339.	0.4	3
608	Thermal Functionalization of Hydrogen-Terminated Porous Silicon Surfaces with Terminal Alkenes and Aldehydes. Materials Research Society Symposia Proceedings, 2000, 638, 1.	0.1	3
609	A quantitative method to discriminate between non-specific and specific lectin–glycan interactions on silicon-modified surfaces. Journal of Colloid and Interface Science, 2016, 464, 198-205.	9.4	3
610	Graphite oxide catalyzed synthesis of \$eta \$-amino alcohols by ring-opening of epoxides. Turkish Journal of Chemistry, 2017, 41, 70-79.	1.2	3
611	Nanoscale materials for the treatment of water contaminated by bacteria and viruses. , 2020, , 261-305.		3
612	Diaryl Sulfide Derivatives as Potential Iron Corrosion Inhibitors: A Computational Study. Molecules, 2021, 26, 6312.	3.8	3

#	Article	IF	CITATIONS
613	Impact of colistin and colistin-loaded on alginate nanoparticles on pigs infected with a colistin-resistant enterotoxigenic Escherichia coli strain. Veterinary Microbiology, 2022, 266, 109359.	1.9	3
614	Phytic acid-doped poly- <i>N</i> -phenylglycine potato peels for removal of anionic dyes: investigation of adsorption parameters. New Journal of Chemistry, 2022, 46, 5111-5120.	2.8	3
615	Electrocatalytic hydrogen generation using tripod containing pyrazolylborate-based copper( <scp>ii</scp> ), nickel( <scp>ii</scp> ), and iron( <scp>iii</scp> ) complexes loaded on a glassy carbon electrode. RSC Advances, 2022, 12, 8030-8042.	3.6	3
616	Effective PDT/PTT dual-modal phototherapeutic killing of bacteria by using poly(N-phenylglycine) nanoparticles. Mikrochimica Acta, 2022, 189, 150.	5.0	3
617	Preparation of nanowires on free-standing boron-doped diamond films for high performance micro-capacitors. Electrochimica Acta, 2022, 421, 140500.	5.2	3
618	Photoluminescence quenching of chemically functionalized porous silicon by a ruthenium cluster. Physica Status Solidi A, 2003, 197, 476-481.	1.7	2
619	Bovine serum albumin adsorption on functionalized porous silicon surfaces. , 2004, 5578, 99.		2
620	Thermal and photochemical isomerization of exocyclic 1,3-dienes: 1,1-diphenyl-3,4-bis(trimethylsilylmethylene)-1-silacyclopentane s-cis(E,E). Journal of Organometallic Chemistry, 2005, 690, 1028-1032.	1.8	2
621	Organic monolayers as resist layers for Cu deposition on Si (111) surfaces. Journal of Electroceramics, 2006, 16, 71-77.	2.0	2
622	Theoretical and experimental study of the short and long range sensing using gold nanostructures. , 2010, , .		2
623	pHâ€responsive phenylboronic acidâ€modified diamond particles: Switch in carbohydrate capture ability triggers modulation of physicochemical and lectinâ€recognition properties. Physica Status Solidi (A) Applications and Materials Science, 2016, 213, 2124-2130.	1.8	2
624	Carbon-Based Nanostructures for Matrix-Free Mass Spectrometry. Carbon Nanostructures, 2016, , 331-356.	0.1	2
625	Diamond Nanowires: A Recent Success Story for Biosensing. Springer Series on Chemical Sensors and Biosensors, 2017, , 1-18.	0.5	2
626	Near-Infrared Photothermal Heating With Gold Nanostructures. , 2018, , 500-510.		2
627	Graphene-Based Photocatalytic Materials for Conversion of Carbon Dioxide to Solar Fuels. , 2018, , 396-412.		2
628	Synthesis and photocatalytic efficiency of sol-gel Al3+-doped TiO2 thin films: correlation between the structural, morphological and optical properties. Materials Research Express, 2019, 6, 085036.	1.6	2
629	In Situ Chemical Modification of Peptide Microarrays: Characterization by Desorption/Ionization on Silicon Nanowires. Methods in Molecular Biology, 2010, 669, 125-133.	0.9	2
630	Efficient and Regioselective Ring-opening of Epoxides with Carboxylic Acid Catalyzed by Graphite Oxide. Letters in Organic Chemistry, 2020, 17, 532-538.	0.5	2

#	Article	IF	CITATIONS
631	A newly synthesized bipyridineâ€containing manganese( <scp>II</scp> ) complex immobilized on graphene oxide as active electrocatalyst for hydrogen gas production from alkaline solutions: Experimental and theoretical studies. International Journal of Energy Research, 2022, 46, 6577-6593.	4.5	2
632	Fullerene―C 60 / NH 2 : A recyclable heterogeneous catalyst for the green synthesis of chromene and pyrimidine derivatives and antibacterial evaluation. Journal of Heterocyclic Chemistry, 0, , .	2.6	2
633	Cathodic Activation of Titania-Fly Ash Cenospheres for Efficient Electrochemical Hydrogen Production: A Proposed Solution to Treat Fly Ash Waste. Catalysts, 2022, 12, 466.	3.5	2
634	Enhancing Colistin Activity against Colistin-Resistant Escherichia coli through Combination with Alginate Nanoparticles and Small Molecules. Pharmaceuticals, 2022, 15, 682.	3.8	2
635	Influence of graphene oxide on the toxicity of polystyrene nanoplastics to the marine microalgae Picochlorum sp Environmental Science and Pollution Research, 2022, 29, 75870-75882.	5.3	2
636	Enhanced Antibacterial Activity of Dermaseptin through Its Immobilization on Alginate Nanoparticles—Effects of Menthol and Lactic Acid on Its Potentialization. Antibiotics, 2022, 11, 787.	3.7	2
637	PALLADIUM CHLORIDE-CATALYZED SYNTHESIS OF 1-X-1-ALKYL (OR 1-ARYL)-1-SILACYCLOPENT-3-ENES ( X = Cl,)	Tj ETQq1	1 0.784314 r 1
638	Clicking ferrocene to halogenated boron-doped diamond surfaces. Rare Metals, 2013, 32, 100-104.	7.1	1
639	Synthesis and Functional Coating of Nanostructured Silicon as an Effective Substrate for Laser Desorption/Ionization Mass Spectrometry. Journal of Nanoscience and Nanotechnology, 2016, 16, 7994-7998.	0.9	1
640	The multiple effects of organoclay and solvent evaporation on hydrophobicity of composite surfaces. Turkish Journal of Chemistry, 2017, 41, 793-801.	1.2	1
641	Aqueous medium-induced micropore formation in plasma polymerized polystyrene: an effective route to inhibit bacteria adhesion. Journal of Materials Chemistry B, 2018, 6, 3674-3683.	5.8	1
642	662 Bacterial infection and wound healing in an ex vivo human skin model. Journal of Investigative Dermatology, 2019, 139, S328.	0.7	1
643	LB1138 An ex vivo human skin model for healing of infected wounds. Journal of Investigative Dermatology, 2019, 139, B24.	0.7	1
644	Au-assisted Polymerization of Conductive Poly(N-phenylglycine) as High-performance Positive Electrodes for Asymmetric Supercapacitors. Nanotechnology, 2021, 33, .	2.6	1
645	Surface modification of silicon nanowires for biosensing. , 2022, , 25-68.		1
646	Plasmonic Photothermal Therapy with Gold Nanorods/Reduced Graphene Oxide Core/Shell Nanocomposites. , 2015, , 1-8.		1
647	Palladium-Catalyzed Reduction of Olefins with Triethylsilane ChemInform, 2003, 34, no.	0.0	0
648	Palladium-Catalyzed Protection of Alcohols and Cleavage of Triethylsilyl Ethers ChemInform, 2005, 36, no.	0.0	0

#	Article	IF	CITATIONS
649	Photoluminescence quenching of colloidal silver nanoparticle on porous silicon. , 2005, , .		0
650	Colloidal Silver Nanoparticle Induced Photoluminescence Quench on the Surface Functionalized Planar Si. Materials Research Society Symposia Proceedings, 2005, 901, 1.	0.1	0
651	Protein Adsorption on the Surface Functionalized Planar Si. Materials Research Society Symposia Proceedings, 2005, 901, 1.	0.1	0
652	Synthesis and Optical Properties of Silicon Oxide Nanowires. Materials Research Society Symposia Proceedings, 2006, 958, 1.	0.1	0
653	Properties of Pt-Assisted Electroless Etched Silicon in HF/Na <sub>2</sub> S <sub>2</sub> O <sub>8</sub> Solution. Materials Science Forum, 0, 609, 231-237.	0.3	0
654	Template assisted highly ordered novel self assembly of micro-reservoirs and its replication. Lab on A Chip, 2010, 10, 1902.	6.0	0
655	Enhanced gold film-coupled graphene-based plasmonic nanosensor. Proceedings of SPIE, 2013, , .	0.8	0
656	Droplet based lab-on-chip microfluidic Microsystems integrated nanostructured surfaces for high sensitive mass spectrometry analysis. , 2013, , .		0
657	Porous Silicon-Based Mass Spectrometry. , 2014, , 1-16.		0
658	Silicon Nanostructures-Graphene Nanocomposites. Advances in Chemical and Materials Engineering Book Series, 2014, , 176-195.	0.3	0
659	Morphological and Optical Properties of Stain Etched Silicon in Vanadium Oxide (V2O5) / Hydrofluoric Acid (HF) Solution. ECS Transactions, 2015, 69, 87-93.	0.5	0
660	Graphene-Microbial Interactions. , 2017, , 289-314.		0
661	Plasmon-induced photocatalytic transformations. , 2020, , 249-275.		0
662	Natural antibodies: Protecting role of IgM in glioblastoma and brain tumours. Current Pharmaceutical Design, 2021, 27, 4515-4529.	1.9	0
663	Biocompatibility of semiconducting silicon nanowires. , 2022, , 69-110.		0
664	Surface and Superlattice. Nanostructure Science and Technology, 2009, , 71-102.	0.1	0
665	Metal Oxide-Graphene Nanocomposites. Advances in Chemical and Materials Engineering Book Series, 2014, , 196-225.	0.3	0
666	CHAPTER 4. Peroxynitrite-Sensitive Electrochemically Active Matrices. RSC Detection Science, 2015, , 63-77.	0.0	0

#	Article	IF	CITATIONS
667	Plasmonic Photothermal Therapy with Gold Nanorods/Reduced Graphene Oxide Core/Shell Nanocomposites. , 2016, , 3287-3294.		0
668	Porous Silicon Based Mass Spectrometry. , 2018, , 1-17.		0
669	Porous Silicon Based Mass Spectrometry. , 2018, , 1337-1353.		0
670	Electrochemical H2 Production using Polypyrazole based Zinc(II) Complex in Alkaline Medium. Asian Journal of Chemistry, 2022, 34, 1366-1372.	0.3	0